Exact General Relativistic Perfect Fluid Disks with Halos

Daniel Vogt*
Instituto de Física Gleb Wataghin, Universidade Estadual de Campinas 13083-970 Campinas, S.P., Brazil

Patricio. S. Letelier†
Departamento de Matemática Aplicada-IMECC, Universidade Estadual de Campinas, 13081-970 Campinas, S.P., Brazil

Using the well-known "displace, cut and reflect" method used to generate disks from given solutions of Einstein field equations, we construct static disks made of perfect fluid based on vacuum Schwarzschild's solution in isotropic coordinates. The same method is applied to different exact solutions to the Einstein's equations that represent static spheres of perfect fluids. We construct several models of disks with axially symmetric perfect fluid halos.

All disks have some common features: surface energy density and pressures decrease monotonically and rapidly with radius. As the "cut" parameter a decreases, the disks become more relativistic, with surface energy density and pressure more concentrated near the center. Also regions of unstable circular orbits are more likely to appear for high relativistic disks. Parameters can be chosen so that the sound velocity in the fluid and the tangential velocity of test particles in circular motion are less then the velocity of light. This tangential velocity first increases with radius and reaches a maximum.

PACS numbers: numbers: 04.20.Jb, 04.40.-b, 97.10.Gz

I. INTRODUCTION

Axially symmetric solutions of Einstein's field equations corresponding to disklike configurations of matter are of great astrophysical interest, since they can be used as models of galaxies or accretion disks. These solutions can be static or stationary and with or without radial pressure. Solutions for static disks without radial pressure were first studied by Bonnor and Sackfield [1], and Morgan and Morgan [2], and with radial pressure by Morgan and Morgan [3]. Disks with radial tension have been considered in [4], and models of disks with electric fields [5], magnetic fields [6], and both magnetic and electric fields have been introduced recently [7]. Solutions for self-similar static disks were analyzed by Lynden-Bell and Pineault [8], and Lemos [9]. The superposition of static disks with black holes were considered by Lemos and Letelier [10, 11, 12], and Klein [13]. Also Bičák, Lynden-Bell and Katz [14] studied static disks as sources of known vacuum spacetimes and Bičák, Lynden-Bell and Pichon [15] found an infinity number of new static solutions. For a recent survey on relativistic gravitating disks, see [16].

The principal method to generate the above mentioned solution is the "displace, cut and reflect" method. One of the main problem of the solutions generated by using this simple method is that usually the matter content of the disk is anisotropic i.e., the radial pressure is different from the azimuthal pressure. In most of the solutions the radial pressure is null. This made these solutions rather unphysical. Even though, one can argue that when no radial pressure is present stability can be achieved if we have two circular streams of particles moving in opposite directions (counter rotating hypothesis, see for instance [14]).

In this article we apply the "displace, cut and reflect" method on spherically symmetric solutions of Einstein's field equations in isotropic coordinates to generate static disks made of a *perfect fluid*, i.e., with radial pressure equal to tangential pressure and also disks of perfect fluid surrounded by an halo made of perfect fluid matter.

The article is divided as follows. Section II gives an overview of the "displace, cut and reflect" method. Also we present the basic equations used to calculate the main physical variables of the disks. In section III we apply the formalism to obtain the simplest model of disk, that is based on Schwarzschild's vacuum solution in isotropic coordinate. The generated class of disks is made of a perfect fluid with well behaved density and pressure. Section IV presents some models of disks with halos obtained from different known exact solutions of Einstein's field equations for static spheres of perfect fluid in isotropic coordinates. In section V we give some examples of disks with halo generated from spheres composed of fluid layers. Section VI is devoted to discussion of the results.

* e-mail: danielvt@ifi.unicamp.br
† e-mail: letelier@ime.unicamp.br

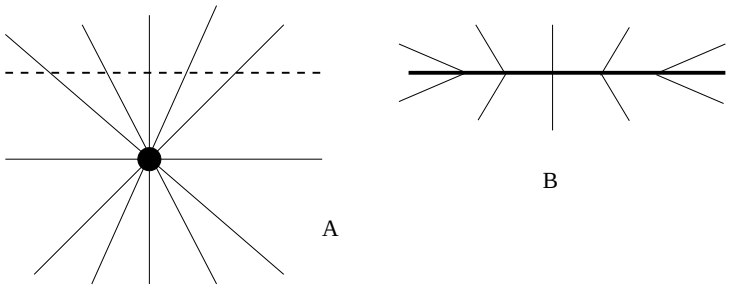

FIG. 1: An illustration of the "displace, cut and reflect" method for the generation of disks. In A the spacetime with a singularity is displaced and cut by a plane (dotted line), in B the part with singularities is disregarded and the upper part is reflected on the plane.

II. EINSTEIN EQUATIONS AND DISKS

For a static spherically symmetric spacetime the general line element in isotropic spherical coordinates can be cast as,

$$\mathrm{d}s^2 = e^{\nu(r)}\mathrm{d}t^2 - e^{\lambda(r)}\left[\mathrm{d}r^2 + r^2(\mathrm{d}\theta^2 + \sin^2\theta\mathrm{d}\varphi^2)\right]. \tag{1}$$

In cylindrical coordinates (t,R,z,φ) the line element (1) takes the form,

$$\mathrm{d}s^2 = e^{\nu(R,z)}\mathrm{d}t^2 - e^{\lambda(R,z)}\left(\mathrm{d}R^2 + \mathrm{d}z^2 + R^2\mathrm{d}\varphi^2\right). \tag{2}$$

The metric of the disk will be constructed using the well known "displace, cut and reflect" method that was used by Kuzmin [17] in Newtonian gravity and later in general relativity by many authors [4]-[16]. The material content of the disk will be described by functions that are distributions with support on the disk. The method can be divided in the following steps that are illustrated in Fig. 1: First, in a space wherein we have a compact source of gravitational field, we choose a surface (in our case, the plane $z = 0$) that divides the space in two pieces: one with no singularities or sources and the other with the sources. Then we disregard the part of the space with singularities and use the surface to make an inversion of the nonsingular part of the space. This results in a space with a singularity that is a delta function with support on $z = 0$. This procedure is mathematically equivalent to make the transformation $z \to |z| + a$, with a constant. In the Einstein tensor we have first and second derivatives of z. Since $\partial_z|z| = 2\vartheta(z) - 1$ and $\partial_{zz}|z| = 2\delta(z)$, where $\vartheta(z)$ and $\delta(z)$ are, respectively, the Heaviside function and the Dirac distribution. Therefore the Einstein field equations will separate in two different pieces [18]: one valid for $z \neq 0$ (the usual Einstein's equations), and other involving distributions with an associated energy-momentum tensor, $T_{ab} = Q_{ab}\delta(z)$, with support on $z = 0$. For the metric (2), the non-zero components of Q_{ab} are

$$Q^t_t = \frac{1}{16\pi}\left[-b^{zz} + g^{zz}(b^R_R + b^z_z + b^\varphi_\varphi)\right], \tag{3}$$

$$Q^R_R = Q^\varphi_\varphi = \frac{1}{16\pi}\left[-b^{zz} + g^{zz}(b^t_t + b^R_R + b^z_z)\right], \tag{4}$$

where b_{ab} denote the jump of the first derivatives of the metric tensor on the plane $z = 0$,

$$b_{ab} = g_{ab,z}|_{z=0^+} - g_{ab,z}|_{z=0^-}, \tag{5}$$

and the other quantities are evaluated at $z = 0^+$. The "true" surface energy-momentum tensor of the disk can be written as $S_{ab} = \sqrt{-g_{zz}}Q_{ab}$, thus the surface energy density σ and the radial and azimuthal pressures or tensions (P) read:

$$\sigma = \sqrt{-g_{zz}}Q^t_t, \quad P = -\sqrt{-g_{zz}}Q^R_R = -\sqrt{-g_{zz}}Q^\varphi_\varphi. \tag{6}$$

Note that when the same procedure is applied to an axially symmetric spacetime in Weyl coordinates we have $Q^R_R = 0$, i.e., we have no radial pressure or tension.

This procedure in principle can be applied to any spacetime solution of the Einstein equations with or without source (stress tensor). The application to a static sphere of perfect fluid is schematized in Fig. 2. The sphere is displaced and cut by a distance a less then its radius r_b. The part of the space that contains the center of the sphere

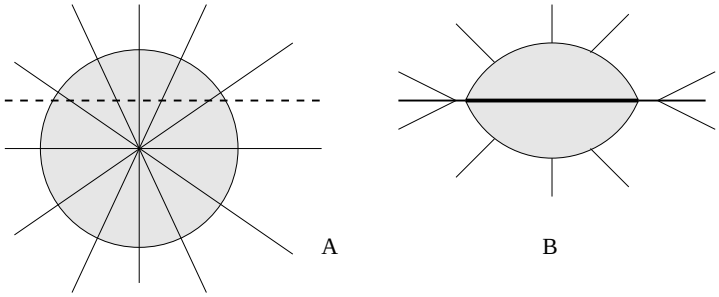

FIG. 2: An illustration of the "displace, cut and reflect" method for the generation of disks with halos. In A the sphere of perfect fluid is displaced and cut by a plane (dotted line), in B the lower part is disregarded and the upper part is reflected on the plane.

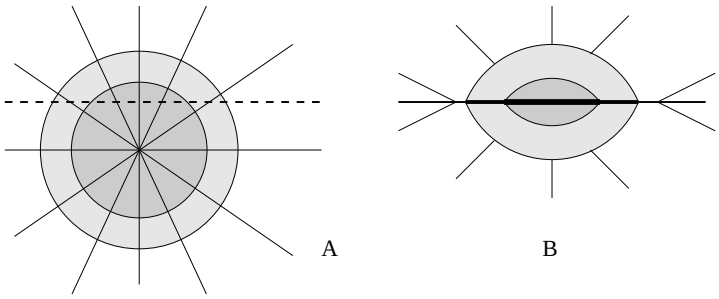

FIG. 3: An illustration of the "displace, cut and reflect" method for the generation of disks with various layers of halos. In A the sphere with different layers of fluid is displaced and cut with a plane (dotted line), in B the field is reflected on the plane.

is disregarded. After the inversion of the remaining space, we end up with a disk surrounded by a cap of perfect fluid. The properties of the inner part of the disk will depend on the internal fluid solution, but if the internal spherical fluid solution is joined to the standard external Schwarzschild solution, the physical properties of the outer part of the disk will be those originated from Schwarzschild's vacuum solution.

In isotropic coordinates the matching at the boundary of the fluid sphere leads to four continuity conditions metric functions e^{λ} and e^{ν} together with their first derivatives with respect to the radial coordinate should be continuous across the boundary. In addition, to have a compact body the pressure at the surface of the material sphere has to drop to zero. Also to have a meaningfully solution the velocity of sound, $\mathrm{V}^2 = \frac{dp}{d\rho}$ should be restricted to the interval $0 \leq \mathrm{V} < 1$.

The Einstein equations for a static spherically symmetric space time in isotropic coordinates for a perfect fluid source give us that density ρ and pressure p are related to the metric functions by

$$\rho = -\frac{e^{-\lambda}}{8\pi}\left[\lambda'' + \frac{1}{4}(\lambda')^2 + \frac{2\lambda'}{r}\right], \tag{7}$$

$$p = \frac{e^{-\lambda}}{8\pi}\left[\frac{1}{4}(\lambda')^2 + \frac{1}{2}\lambda'\nu' + \frac{1}{r}(\lambda' + \nu')\right], \tag{8}$$

where primes indicate differentiation with respect to r.

Also static spheres composed of various layers of fluid can be used to generate disks with halos of fluid layers (see figure 3). The disk will then be composed of different axial symmetric "pieces" glued together. The matching conditions at the boundary of adjacent spherical fluid layers in isotropic coordinates involves four continuity conditions: the two metric functions e^{λ} and e^{ν}, the first derivative of λ with respect to the radial coordinate, and the pressure should be continuous across the boundary. At the most external boundary, the metric functions e^{λ} and e^{ν}, and their first derivatives with respect to the radial coordinate should be continuous across the boundary; also the pressure there should go to zero.

III. THE SIMPLEST DISK

We first apply the "displace, cut and reflect" method to generate disks discussed in the previous section and depicted in Fig. 1 to the Schwarzschild metric in isotropic coordinates (t, r, θ, φ),

$$\mathrm{d}s^2 = \frac{\left(1-\frac{m}{2r}\right)^2}{\left(1+\frac{m}{2r}\right)^2}\mathrm{d}t^2 - \left(1+\frac{m}{2r}\right)^4\left[\mathrm{d}r^2 + r^2(\mathrm{d}\theta^2 + \sin^2\theta \mathrm{d}\varphi^2)\right]. \tag{9}$$

Expressing solution (9) in cylindrical coordinates, and using Eq. (3) – (6), we obtain a disk with surface energy density σ and radial and azimuthal pressures (or tensions) P given by

$$\sigma = \frac{4ma}{\pi(m+2\sqrt{R^2+a^2})^3}, \tag{10}$$

$$P = -\frac{2m^2a}{\pi(m+2\sqrt{R^2+a^2})^3(m-2\sqrt{R^2+a^2})}. \tag{11}$$

The total mass of the disk can be calculated with the help of Eq. (10):

$$\mathcal{M} = \int_0^\infty\int_0^{2\pi} \sigma\sqrt{g_{RR}g_{\varphi\varphi}}\,\mathrm{d}R\,\mathrm{d}\varphi = \frac{m}{4a}(m+4a). \tag{12}$$

Eq. (10) shows that the disk's surface energy density is always positive (weak energy condition). Positive values (pressure) for the stresses in azimuthal and radial directions are obtained if $m < 2\sqrt{R^2+a^2}$. The strong energy condition, $\sigma + P_{\varphi\varphi} + P_{RR} = \sigma + 2P > 0$ is then satisfied. These properties characterize a fluid made of matter with the usual gravitational attractive property. This is not a trivial property of these disks since it is known that the "displace, cut and reflect" method sometimes gives disks made of exotic matter like cosmic strings, see for instance [19].

Another useful parameter is the velocity of sound propagation V, defined as $V^2 = \frac{dP}{d\sigma}$, which can be calculated using Eq. (10) and Eq. (11):

$$V^2 = \frac{m(4\sqrt{R^2+a^2}-m)}{3(m-2\sqrt{R^2+a^2})^2}. \tag{13}$$

The condition $V^2 < 1$ (no tachyonic matter) imposes the inequalities $m < \sqrt{R^2+a^2}$ or $m > 3\sqrt{R^2+a^2}$. If the pressure condition and the speed of sound less then the speed of light condition are to be simultaneously satisfied, then $m < \sqrt{R^2+a^2}$. This inequality will be valid in all the disk if $m < a$.

With the presence of radial pressure one does not need the assumption of streams of rotating and counter rotating matter usually used to explain the stability of static disk models. However, a tangential velocity (rotation profile) can be calculated by assuming a test particle moves in a circular geodesic on the disk. We tacitly assume that this particle only interact gravitationally with the fluid. This assumption is valid for the case of a particle moving in a very diluted gas like the gas made of stars that models a galaxy disk.

The geodesic equation for the R coordinate obtained from metric (2) is

$$e^\lambda\ddot{R} + \frac{1}{2}(e^\nu)_{,R}\dot{t}^2 - \frac{1}{2}(e^\lambda)_{,R}(\dot{R}^2+\dot{z}^2) - \frac{1}{2}\left(e^\lambda R^2\right)_{,R}\dot{\varphi}^2 = 0. \tag{14}$$

For circular motion on the $z=0$ plane, $\dot{R} = \ddot{R} = 0$ and $\dot{z} = 0$, then Eq. (14) reduces to

$$\frac{\dot{\varphi}^2}{\dot{t}^2} = \frac{(e^\nu)_{,R}}{(e^\lambda R^2)_{,R}}. \tag{15}$$

The tangential velocity measured by an observer at infinity is then

$$\mathrm{v}_c^2 = -\frac{g_{\varphi\varphi}}{g_{tt}}\left(\frac{d\varphi}{dt}\right)^2 = R^2\frac{e^\lambda(e^\nu)_{,R}}{e^\nu(R^2e^\lambda)_{,R}}. \tag{16}$$

From the metric on the disk,

$$e^\nu = \frac{\left(1-\frac{m}{2\sqrt{R^2+a^2}}\right)^2}{\left(1+\frac{m}{2\sqrt{R^2+a^2}}\right)^2} \quad \text{and} \quad e^\lambda = \left(1+\frac{m}{2\sqrt{R^2+a^2}}\right)^4, \tag{17}$$

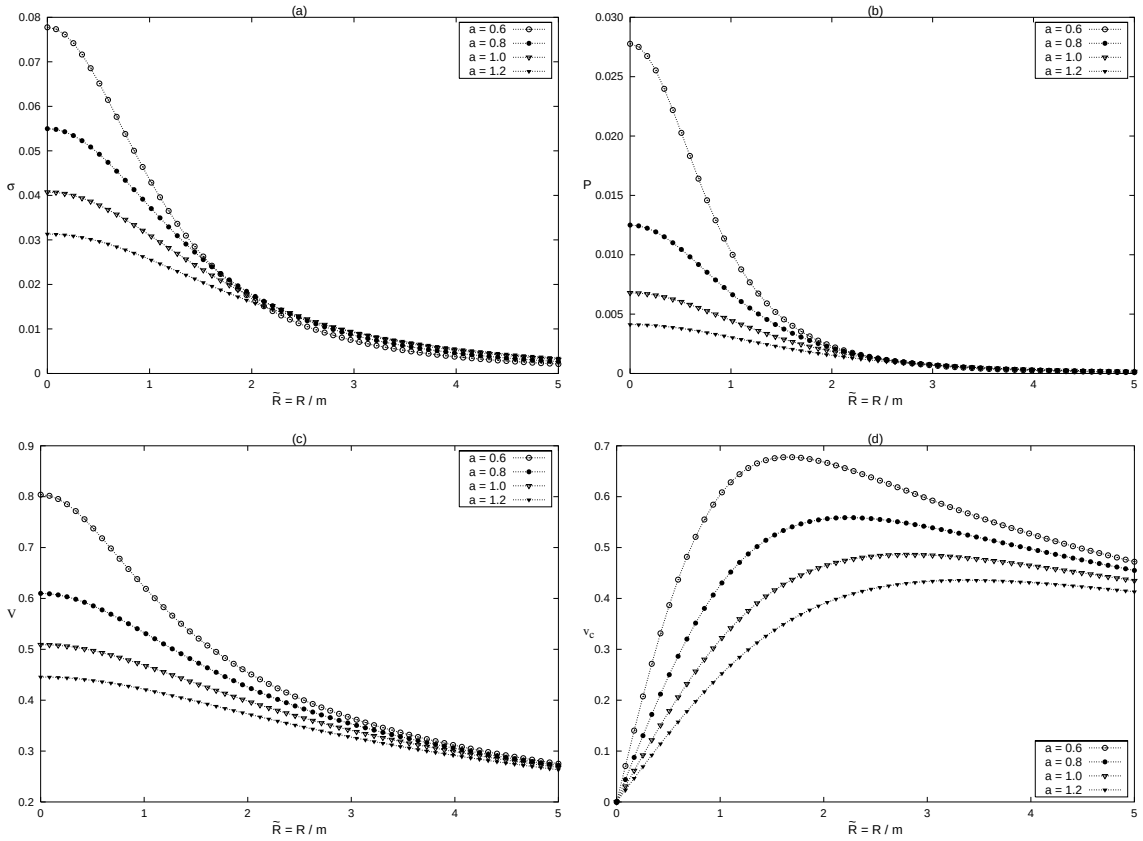

FIG. 4: (a) The surface energy density σ, (b) pressures P, (c) sound velocity V and (d) tangential velocity v_c (rotation curve or rotation profile) with $m = 0.5$ and $a = 0.6$, 0.8, 1.0, and 1.2 as function of $\tilde{R} = R/m$. We use geometric units $G = c = 1$.

we find that Eq. (16) can be cast as,

$$\mathrm{v}_c^2 = \frac{mR^2}{\left(1 - \frac{m}{2\sqrt{R^2+a^2}}\right)\left[(R^2+a^2)^{3/2} + \frac{m}{2}(a^2 - R^2)\right]}. \tag{18}$$

For $R >> a$, Eq. (18) goes as $\mathrm{v}_c = (m/R)^{1/2}$, the Newtonian circular velocity.

To determine the stability of circular orbits on the disk's plane, we use an extension of Rayleigh [20, 21] criteria of stability of a fluid at rest in a gravitational field

$$h\frac{dh}{dR} > 0, \tag{19}$$

where h is the specific angular momentum of a particle on the disk's plane:

$$h = -g_{\varphi\varphi}\frac{d\varphi}{ds} = -g_{\varphi\varphi}\frac{d\varphi}{dt}\frac{dt}{ds}. \tag{20}$$

Using Eq. (15) and the relation

$$1 = e^{\nu}\left(\frac{dt}{ds}\right)^2 - R^2 e^{\lambda}\left(\frac{d\varphi}{ds}\right)^2, \tag{21}$$

one obtains the following expression for h:

$$h = R^2 e^{\lambda}\sqrt{\frac{(e^{\nu})_{,R}}{e^{\nu}(R^2 e^{\lambda})_{,R} - R^2 e^{\lambda}(e^{\nu})_{,R}}}. \tag{22}$$

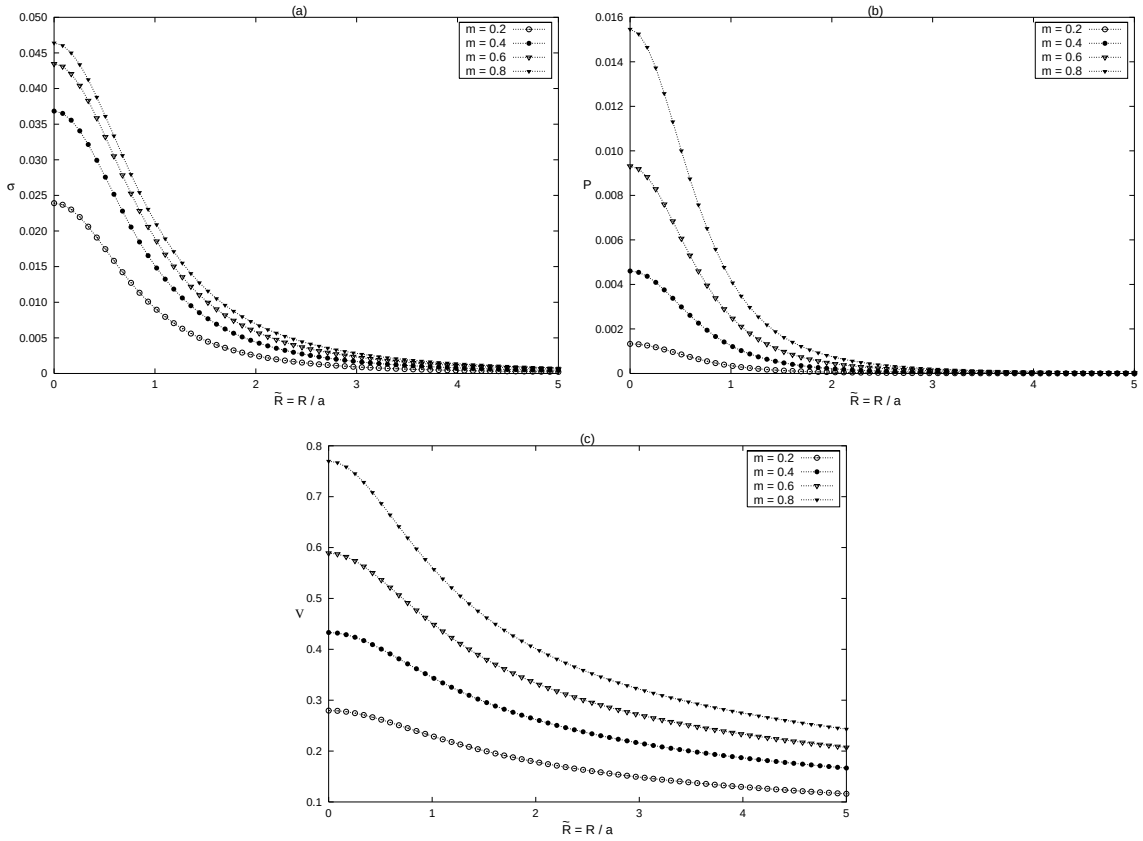

FIG. 5: (a) The surface energy density σ, (b) pressures P and (c) sound velocity V with $a = 1.0$ and $m = 0.2$, 0.4, 0.6, and 0.8 as function of $\tilde{R} = R/a$.

For the functions (17), Eq. (22) reads

$$h = \frac{2\sqrt{m}R^2\left(1+\frac{m}{2\sqrt{R^2+a^2}}\right)^2(R^2+a^2)^{1/4}}{\sqrt{4(R^2+a^2)^2 - 8mR^2\sqrt{R^2+a^2}+m^2(R^2-a^2)}}. \tag{23}$$

The stability criterion is always satisfied for $\frac{a}{m} \gtrapprox 1.016$.

In figure 4 (a)–(d) we show, respectively, the surface energy density, pressures, the sound velocity and curves of the tangential velocity (rotation curves) Eq. (18) with $m = 0.5$ and $a = 0.6$, 0.8, 1.0, and 1.2 as functions of $\tilde{R} = R/m$. Figure 5 (a)–(c) display, respectively, the surface energy density, pressures and sound velocity with parameters $a = 1.0$ and $m = 0.2$, 0.4, 0.6, 0.8 as as functions of $\tilde{R} = R/m$. We see that the first three quantities decrease monotonically with the radius of the disk, as can be checked from Eq. (10), (11) and (13). Energy density decreases rapidly enough to, in principle, define a cut off radius and consider the disk as finite.

IV. DISKS WITH HALOS

Now we study some disks with halos constructed from several exact solutions of the Einstein equations for static spheres of perfect fluid. A survey of these class of solutions is presented in [22].

A. Buchdahl's Solution

The first situation that we shall study is similar to the one depicted in Fig. 2 wherein we start with a sphere of perfect fluid. This case will not be exactly the same as the one presented in the mentioned figure because the sphere has no boundary. Hence the generated disk will be completely immersed in the fluid. An example of exact solution

of the Einstein equations that represent a fluid sphere with no boundary is the the Buchdahl solution that may be regarded as a reasonably close analogue to the classical Lane-Emden index 5 polytrope [23]. The metric functions for this solution are:

$$e^{\nu}=\left(\frac{1-\frac{A}{\sqrt{1+kr^2}}}{1+\frac{A}{\sqrt{1+kr^2}}}\right)^2,\quad e^{\lambda}=\left(1+\frac{A}{\sqrt{1+kr^2}}\right)^4, \tag{24}$$

where A and k are constants. Far from the origin the solution goes over into the external Schwarzschild metric, when $m=\frac{2A}{\sqrt{k}}$. The density, pressure and sound velocity are given by:

$$\rho=\frac{3Ak}{2\pi(A+\sqrt{1+kr^2})^5},\quad p=\frac{kA^2}{2\pi(-A+\sqrt{1+kr^2})(A+\sqrt{1+kr^2})^5}, \tag{25}$$

$$\mathrm{V}^2=\frac{2A(-2A+3\sqrt{1+kr^2})}{15(A-\sqrt{1+kr^2})^2}. \tag{26}$$

The condition $\mathrm{V}<1$ is satisfied for $A<\frac{(18-\sqrt{39})}{19}\sqrt{1+kr^2}$.

Using Eq. (24) and Eqs. (3)–(6), we get the following expressions for the energy density, pressure and sound velocity of the disk:

$$\sigma=\frac{akA}{\pi\left[A+\sqrt{1+k(R^2+a^2)}\right]^3}, \tag{27}$$

$$P=\frac{akA^2}{2\pi\left[-A+\sqrt{1+k(R^2+a^2)}\right]\left[A+\sqrt{1+k(R^2+a^2)}\right]^3}, \tag{28}$$

$$V^2=\frac{A\left[-A+2\sqrt{1+k(R^2+a^2)}\right]}{3\left[A-\sqrt{1+k(R^2+a^2)}\right]^2}. \tag{29}$$

The conditions $V<1$ and $P>0$ are both satisfied if $A<\frac{1}{2}\sqrt{1+ka^2}$. Figure 6 (a)–(d) shows, respectively, σ, P, V and rotation curves, Eq. (30), as functions of $\tilde{R}=R/m$ for the disk calculated from Buchdahl's solution.

In figure 7 (a)–(b) we show, respectively, the density ρ together with pressure p, and sound velocity V of the halo along the axis z for $A=0.6$; $k=1$ and $a=1$. Note that in this solution there is no boundary of the fluid sphere: the disk is completely immersed in the fluid.

The tangential velocity v_c calculated from metric coefficients (24) is

$$\mathrm{v}_c^2=\frac{2AkR^2}{\left(1-A/\sqrt{1+k(R^2+a^2)}\right)\left\{[1+k(R^2+a^2)]^{3/2}+A[1+k(a^2-R^2)]\right\}}. \tag{30}$$

For $R>>a$, Eq. (30) goes as $\mathrm{v}_c=(2A)^{1/2}/(R^{1/2}k^{1/4})$. The specific angular momentum follows from Eq. (22) and Eq. (24):

$$h=\frac{\sqrt{2Ak}R^2\left(1+\frac{A}{\sqrt{1+k(R^2+a^2)}}\right)^2[1+k(R^2+a^2)]^{1/4}}{\sqrt{[1+k(R^2+a^2)]^2-4AkR^2\sqrt{1+k(R^2+a^2)}-A^2[1+k(a^2-R^2)]}}. \tag{31}$$

B. Narlikar-Patwardhan-Vaidya Solutions 1a and 1b

Now we shall study the generation of a disk solution with an halo exactly as the one depicted in Fig. 2. We start with a solution of the Einstein equations in isotropic coordinates that represents a sphere with radius r_b of perfect fluid that on $r=r_b$ will be continuously matched to the vacuum Schwarzschild solution. Narlikar, Patwardhan and Vaidya [24] gave the following two exact solutions of the Einstein equations for a static sphere of perfect fluid characterized by the metric functions (λ,ν_{1a}) and (λ,ν_{1b}),

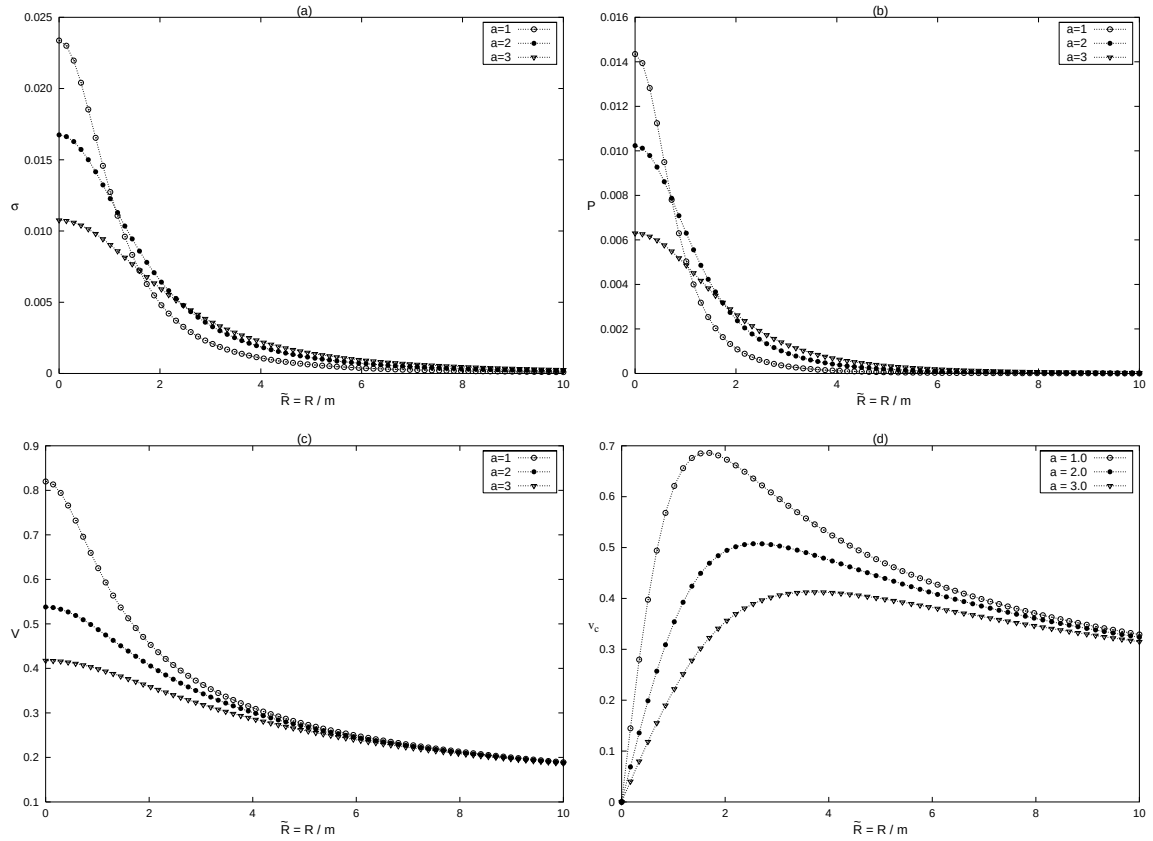

FIG. 6: (a) The surface energy density σ, Eq. (27), (b) the pressure P Eq. (28), (c) the velocity of sound V Eq. (29), (d) the tangential velocity v_c Eq. (30) for the disk with $A = 0.6$; $k = 1$; for $a = 1$, 2 and 3 as function of $\tilde{R} = R/m$.

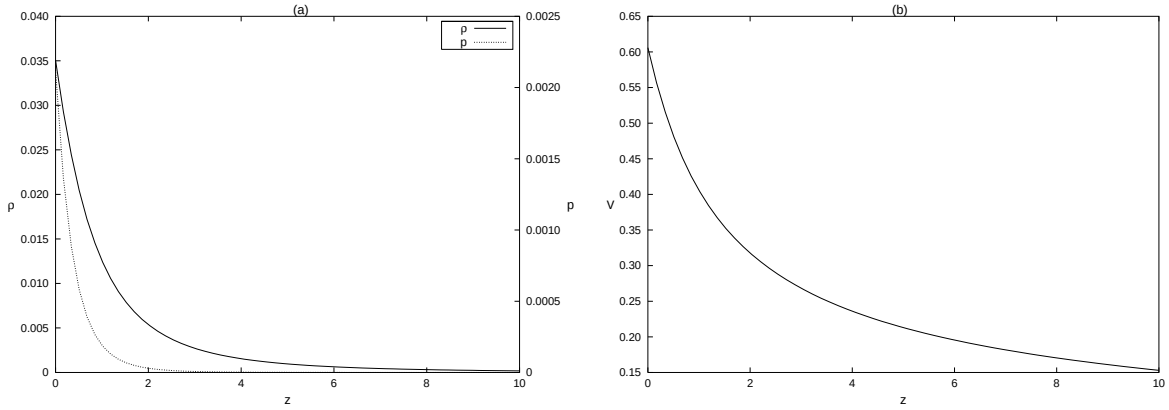

FIG. 7: (a) The density ρ and pressure p Eq. (25) and (b) the velocity of sound V Eq. (26) for the halo with $A = 0.6$; $k = 1$ and $a = 1$ along the axis z.

$$e^{\lambda} = Cr^{k}, \tag{32}$$

$$e^{\nu_{1a}} = \left(A_{1a} r^{1-n+k/2} + B_{1a} r^{1+n+k/2}\right)^2 \quad \text{for } -2+\sqrt{2} < k \leq 0, \tag{33}$$

$$e^{\nu_{1b}} = r^{\sqrt{2}} \left[A_{1b} + B_{1b} \ln(r)\right]^2 \qquad \text{for } k = -2+\sqrt{2}, \tag{34}$$

where A_{1a}, A_{1b}, B_{1a}, B_{1b}, C are constants, and $n = \sqrt{1+2k+k^2/2}$. We shall refer to these solutions as NPV 1a and NPV 1b, respectively.

The density, pressure and sound velocity for for the solutions (λ, ν_{1a}) and (λ, ν_{1b}), will be denoted by (ρ, p_{1a}, V_{1a}) and (ρ, p_{1b}, V_{1b}), respectively. We find,

$$\rho = \frac{-k(k+4)r^{-2-k}}{32\pi C}, \tag{35}$$

$$p_{1a} = \frac{1}{32\pi C r^{2+k}(A_{1a}+B_{1a}r^{2n})}\left\{A_{1a}\left[3k^2+8(1-n)-4k(n-3)\right]\right.$$
$$\left.+B_{1a}\left[3k^2+8(1+n)+4k(n+3)\right]r^{2n}\right\}, \tag{36}$$

$$p_{1b} = \frac{A_{1b}+B_{1b}\ln(r)+2\sqrt{2}B_{1b}}{16\pi C[A_{1b}+B_{1b}\ln(r)]}, \tag{37}$$

$$\mathrm{V}_{1a}^2 = \frac{1}{k(k+4)(A_{1a}+B_{1a}r^{2n})^2}\left\{A_{1a}^2\left[-3k^2+8(n-1)+4k(n-3)\right]\right.$$
$$\left.-B_{1a}^2 r^{4n}\left[3k^2+8(1+n)+4k(n+3)\right]-2A_{1a}B_{1a}r^{2n}\left[3k(k+4)+8(1-n^2)\right]\right\}, \tag{38}$$

$$\mathrm{V}_{1b}^2 = \frac{2B_{1b}^2 r^{\sqrt{2}}}{[A_{1b}+B_{1b}\ln(r)]^2}. \tag{39}$$

The condition of continuity of the metric functions (λ, ν) given by (32)–(34) and the corresponding functions in Eq. (9) at the boundary $r = r_b$ leads to following expressions:

$$\frac{m}{2r_b} = -\frac{k}{k+4}, \quad C = r_b^{-k}\left(\frac{4}{k+4}\right)^4, \tag{40}$$

$$A_{1a} = -\frac{3k^2+8(1+n)+4k(n+3)}{16nr_b^{1-n+k/2}}, \quad B_{1a} = \frac{3k^2+8(1-n)-4k(n-3)}{16nr_b^{1+n+k/2}}, \tag{41}$$

$$A_{1b} = -\frac{2\sqrt{2}+\ln(r_b)}{4r_b^{1/\sqrt{2}}}, \quad B_{1b} = \frac{1}{4r_b^{1/\sqrt{2}}}. \tag{42}$$

V_{1a} has its maximum at $r = 0$, and V_{1b} at $r = r_b$. Condition $\mathrm{V}_{1b}(r_b) < 1$ is satisfied if $r_b < 4^{1/\sqrt{2}}$.

Using Eq. (32)–(34) in Eq. (3)–(6), we get the following expressions for the energy density, pressure and sound velocity of the disk:

$$\sigma = -\frac{ka}{4\pi\sqrt{C}\mathcal{R}^{1+k/4}}, \tag{43}$$

$$P_{1a} = \frac{a}{4\pi\sqrt{C}\mathcal{R}^{1+k/4}}\frac{[A_{1a}(k-n+1)+B_{1a}(k+n+1)\mathcal{R}^n]}{[A_{1a}+B_{1a}\mathcal{R}^n]}, \tag{44}$$

$$P_{1b} = \frac{a}{4\pi\sqrt{C}\mathcal{R}^{1/2+\sqrt{2}/4}[2A_{1b}+B_{1b}\ln(\mathcal{R})]}\left[2A_{1b}(\sqrt{2}-1)+2B_{1b}\right.$$
$$\left.+B_{1b}(\sqrt{2}-1)\ln(\mathcal{R})\right], \tag{45}$$

$$V_{1a}^2 = \frac{1}{k(k+4)\left[A_{1a}\mathcal{R}^{-n/2}+B_{1a}\mathcal{R}^{n/2}\right]^2}\left[-B_{1a}^2\mathcal{R}^n(k^2+5k+nk+4n+4)\right.$$
$$\left.+A_{1a}^2\mathcal{R}^{-n}(-k^2-5k+nk+4n-4)+2A_{1a}B_{1a}(-k^2-5k+4n^2-4)\right], \tag{46}$$

$$V_{1b}^2 = \frac{1}{2(2A_{1b}+B_{1b}\ln(\mathcal{R}))^2}\left[B_{1b}^2\sqrt{2}\ln^2(\mathcal{R})+2B_{1b}(2B_{1b}+B_{1b}\sqrt{2}+2A_{1b}\sqrt{2})\right.$$
$$\left.\times\ln(\mathcal{R})+4A_{1b}B_{1b}(2+\sqrt{2})+4\sqrt{2}A_{1b}^2+8B_{1b}^2\right], \tag{47}$$

where $\mathcal{R} = R^2 + a^2$. V_{1a} and V_{1b} have their maximum values at $R = 0$. Because the expressions are rather involved, the restrictions on the constants to ensure the velocities are positive and less then one is best done graphically. The curves of σ, P and V as function of $\tilde{R} = R/m$ with parameters $k = -1/2$; $r_b = 2$ and $a = 0.5$, 1.0,1.5 are displayed in figure 8 (a)–(c), respectively. Figure 9 (a)–(b) show the density ρ, pressure p and velocity of sound V for the halo with parameters $k = -1/2$; $r_b = 2$, for $a = 0.5$ along the axis z. The same physical quantities are shown in figures 11 (a)–(c) and 12 (a)–(b) with $k = -2+\sqrt{2}$. We note that σ and P are continuous at the boundary between the internal and external parts of the disk, but the velocity of sound has a discontinuity.

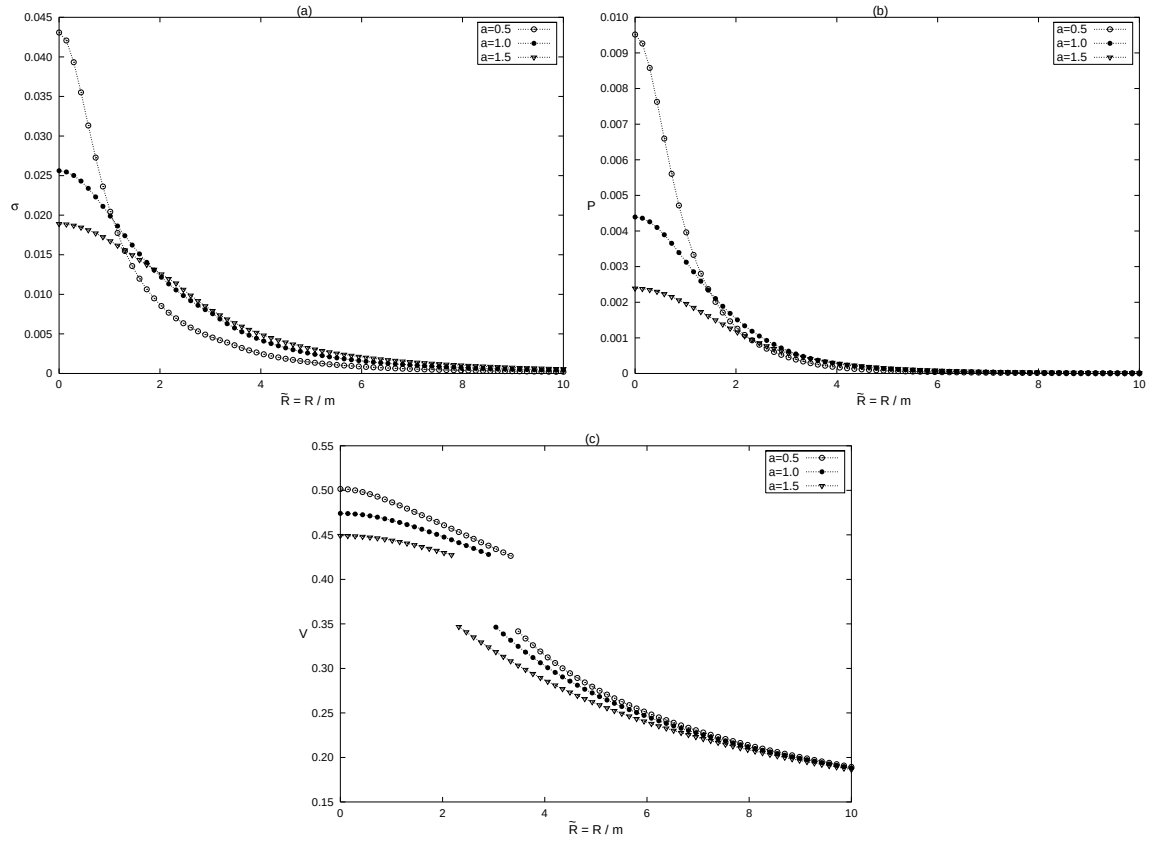

FIG. 8: (a) The surface energy density σ Eq. (43), (b) the pressure P Eq. (44) and (c) the velocity of sound V Eq. (46) for the disk with $\mathbf{k} = -\mathbf{1/2}$; $r_b = 2$; for $a = 0.5$, 1.0 and 1.5 as function of $\tilde{R} = R/m$.

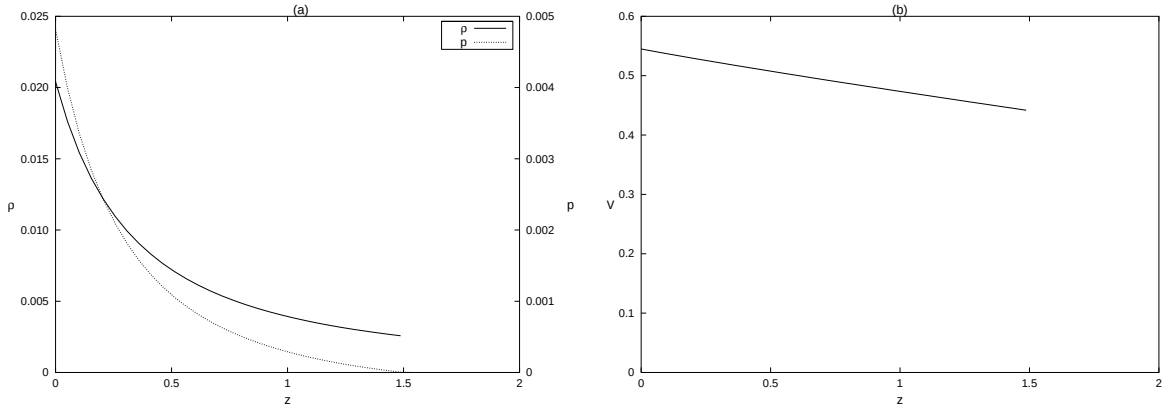

FIG. 9: (a) The density ρ Eq. (35) and pressure p Eq. (36), (b) the velocity of sound V Eq. (38) for the halo with $\mathbf{k} = -\mathbf{1/2}$; $r_b = 2$; for $a = 0.5$ along the axis z.

The tangential velocity v_c is given by

$$\mathrm{v}_{c1a}^2 = 2R^2 \frac{A_{1a}(1-n+k/2) + B_{1a}(1+n+k/2)(R^2+a^2)^n}{[A_{1a} + B_{1a}(R^2+a^2)^n][R^2(k+2)+2a^2]}, \tag{48}$$

$$\mathrm{v}_{c1b}^2 = R^2 \frac{2\sqrt{2}A_{1b} + B_{1b}[4+\sqrt{2}\ln(R^2+a^2)]}{[2A_{1b} + B_{1b}\ln(R^2+a^2)][2a^2+\sqrt{2}R^2]}, \tag{49}$$

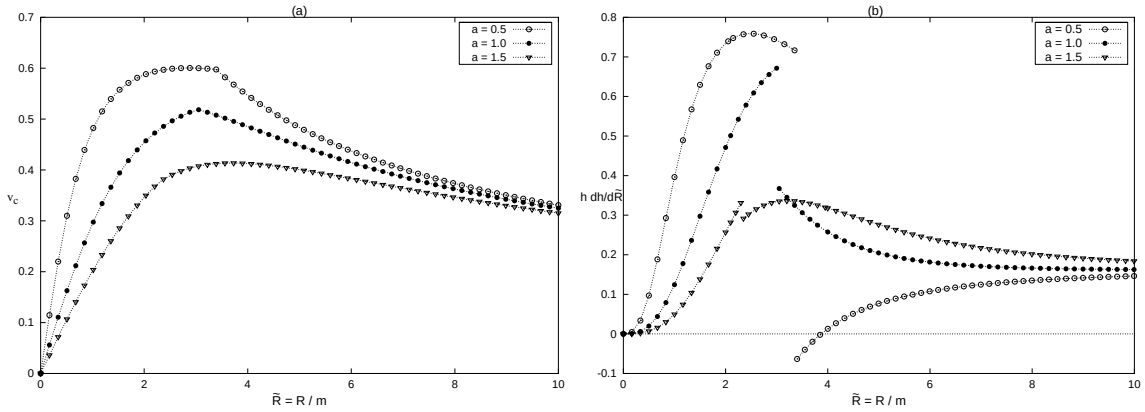

FIG. 10: (a) The tangential velocity v_{c1} Eq. (48) and (b) the curves of $h\frac{dh}{d\tilde{R}}$ Eq. (50) with $\mathbf{k} = -\mathbf{1}/\mathbf{2}$; $r_b = 2$; for $a = 0.5$, 1.0, and 1.5 as function of $\tilde{R} = R/m$. A region of instability appears on the disk generated with parameter $a = 0.5$.

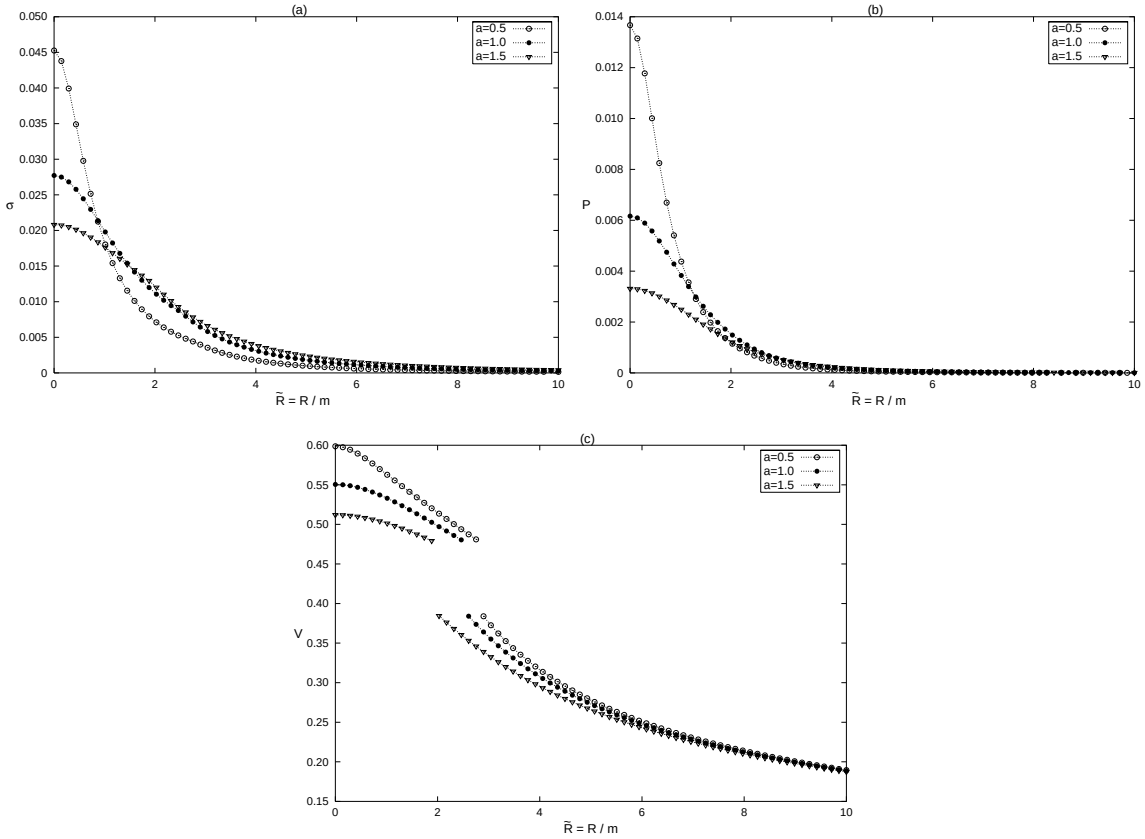

FIG. 11: (a) The surface energy density σ Eq. (43), (b) the pressure P Eq. (45), (c) the velocity of sound V Eq. (47) for the disk with $k = -2 + \sqrt{2}$; $r_b = 2$; for $a = 0.5$, 1.0 and 1.5 as function of $\tilde{R} = R/m$.

and the specific angular momentum h,

$$h_{1a} = \sqrt{C}R^2(R^2+a^2)^{k/4}\sqrt{\frac{A_{1a}(1-n+k/2)+B_{1a}(1+n+k/2)(R^2+a^2)^n}{A_{1a}(a^2+nR^2)+B_{1a}(a^2-nR^2)(R^2+a^2)^n}}, \tag{50}$$

$$h_{1b} = \sqrt{C}R^2(R^2+a^2)^{-1/2+\sqrt{2}/4}\sqrt{\frac{2B_{1b}+\sqrt{2}[A_{1b}+B_{1b}\ln(\sqrt{R^2+a^2})]}{2a^2[A_{1b}+B_{1b}\ln(\sqrt{R^2+a^2})]-2B_{1b}R^2}}. \tag{51}$$

In figure 10 (a)–(b), the curves of tangential velocity Eq. (48) and $h\frac{dh}{d\tilde{R}}$ Eq. (50), respectively, are displayed as

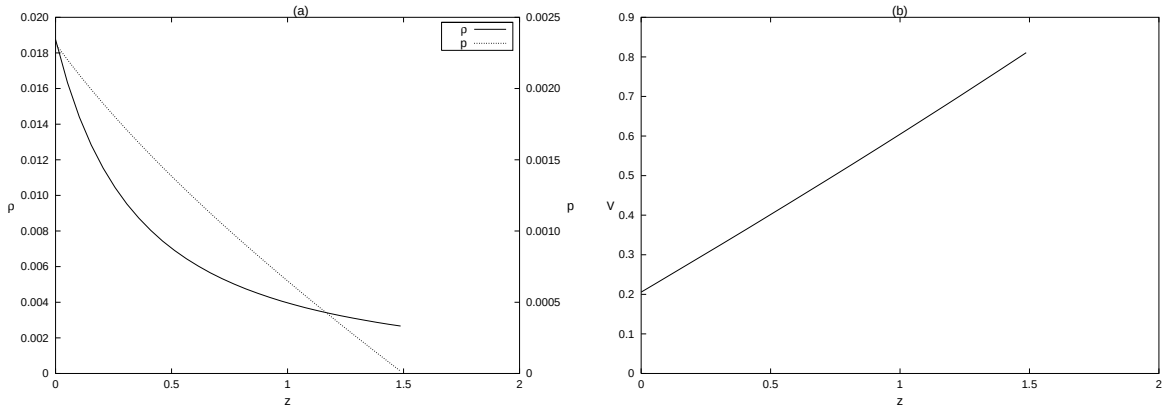

FIG. 12: (a) The density ρ Eq. (35) and pressure p Eq. (37), (b) the velocity of sound V Eq. (39) for the halo with $k = -2+\sqrt{2}$; $r_b = 2$; for $a = 0.5$ along the axis z.

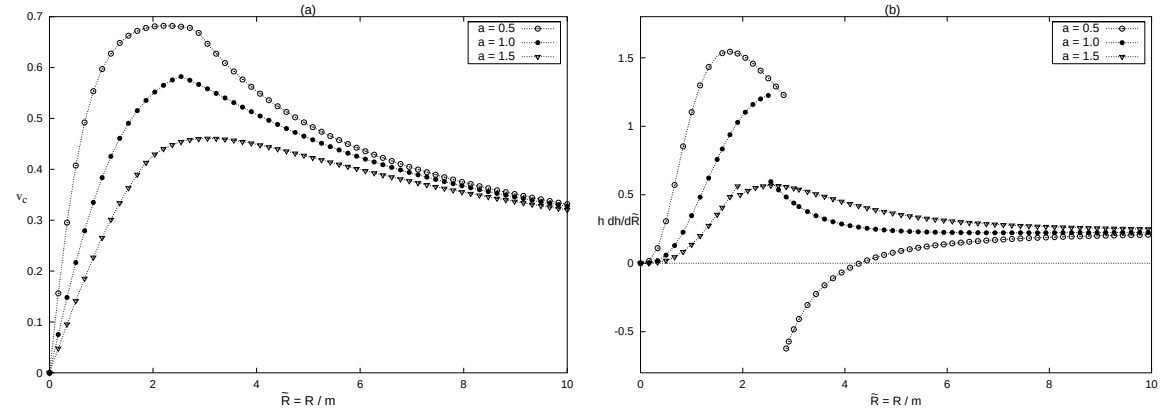

FIG. 13: (a) The tangential velocity v_{c2} Eq. (49), (b) the curves of $h\frac{dh}{d\tilde{R}}$ Eq. (51) with $k = -2+\sqrt{2}$; $r_b = 2$; for $a = 0.5$, 1.0, and 1.5 as function of $\tilde{R} = R/m$. As in the previous case, the same region of instability occurs.

functions of $\tilde{R} = R/m$ with $k = -1/2$; $r_b = 2$; $a = 0.5$, 1.0,1.5. The same quantities are shown in figure 13(a)–(b) with $k = -2+\sqrt{2}$. For $a = 0.5$ the disks have a small region of unstable orbits immediately after the "boundary radius".

C. Narlikar-Patwardhan-Vaidya Solutions 2a and 2b

Like in the previous subsections we study the generation of a disk solution with an halo exactly as the one depicted in Fig. 2. We also start with a solution of the Einstein equations in isotropic coordinates that represents a sphere of radius r_b of perfect fluid that on $r = r_b$ will the continuously matched to the vacuum Schwarzschild solution. We will use another two solutions found by Narlikar, Patwardhan and Vaidya [24] that we shall refer as NPV 2a and NPV 2b, respectivelly. that are characterized by the metric functions (λ, ν_{2a}) and (λ, ν_{2b}),

$$e^{\lambda} = \frac{1}{\left(A_1 r^{1+n/2} + A_2 r^{1-n/2}\right)^2} \tag{52}$$

$$e^{\nu_{2a}} = \frac{\left(B_{1a} r^{1+x/2} + B_{2a} r^{1-x/2}\right)^2}{\left(A_1 r^{1+n/2} + A_2 r^{1-n/2}\right)^2} \quad \text{for } \sqrt{2} < n \leq 2, \tag{53}$$

$$e^{\nu_{2b}} = \frac{[B_{1b} + B_{2b}\ln(r)]^2}{\left(A_1 r^{1/\sqrt{2}} + A_2 r^{-1/\sqrt{2}}\right)^2} \quad \text{for } n = \sqrt{2}. \tag{54}$$

where the A's and B's are constants and $x = \sqrt{2n^2 - 4}$. The solution (λ, ν_{2a}) with $n = 2$ corresponds to Schwarzschild's internal solution in isotropic coordinates (see for instance Ref. [22]). This solution has constant density and is

conformally flat when $B_{1a}=0$.

The density, pressure and sound velocity for the solutions (λ,ν_{2a}) and (λ,ν_{2b}), will be denoted by (ρ,p_{2a},V_{2a}) and (ρ,p_{2b},V_{2b}), respectively. We find,

$$\rho=\frac{1}{32\pi}\left[(4-n^2)\left(A_1r^{n/2}+A_2r^{-n/2}\right)^2+12n^2A_1A_2\right], \tag{55}$$

$$p_{2a}=\frac{1}{32\pi}\left[-12n^2A_1A_2+(3n^2-4)\left(A_1r^{n/2}+A_2r^{-n/2}\right)^2 +\frac{2nx(B_{2a}-B_{1a}r^x)}{B_{2a}+B_{1a}r^x}\left(A_1^2r^n-A_2^2r^{-n}\right)\right], \tag{56}$$

$$p_{2b}=\frac{1}{16\pi(B_{1b}+B_{2b}\ln(r))}\left[(B_{1b}+B_{2b}\ln(r))\left(A_1^2r^{\sqrt{2}}+A_2^2r^{-\sqrt{2}}-10A_1A_2\right) +2\sqrt{2}B_{2b}\left(A_2^2r^{-\sqrt{2}}-A_1^2r^{\sqrt{2}}\right)\right], \tag{57}$$

$$\begin{aligned}\mathrm{V}_{2a}^2=&\frac{1}{(4-n^2)\left(A_1^2r^n-A_2^2r^{-n}\right)(B_{2a}+B_{1a}r^x)^2}\left\{B_{2a}^2\left[A_1^2r^n(3n^2+2nx-4)\right.\right.\\ &\left.+A_2^2r^{-n}(-3n^2+2nx+4)\right]+B_{1a}^2r^{2x}\left[A_1^2r^n(3n^2-2nx-4)\\ &\left.+A_2^2r^{-n}(-3n^2-2nx+4)\right]+2B_{1a}B_{2a}r^x\left[A_1^2r^n(3n^2-2x^2-4)\right.\\ &\left.\left.+A_2^2r^{-n}(-3n^2+2x^2+4)\right]\right\},\end{aligned} \tag{58}$$

$$\begin{aligned}\mathrm{V}_{2b}^2=&\frac{1}{[B_{1b}+B_{2b}\ln(r)]^2\left(A_1^2r^{\sqrt{2}}-A_2^2r^{-\sqrt{2}}\right)}\left\{A_1^2r^{\sqrt{2}}\left[(B_{1b}+B_{2b}\ln(r))\right.\right.\\ &\left.\times(B_{1b}+B_{2b}\ln(r)-2\sqrt{2}B_{2b})+2B_{2b}^2\right]-A_2^2r^{-\sqrt{2}}\\ &\left.\times\left[(B_{1b}+B_{2b}\ln(r))(B_{1b}+B_{2b}\ln(r)+2\sqrt{2}B_{2b})+2B_{2b}^2\right]\right\}.\end{aligned} \tag{59}$$

The condition of continuity of the metric functions (λ,ν) given by (52)–(54) and the corresponding functions in Eq. (9) at the boundary $r=r_b$ leads to following expressions:

$$A_1=\frac{1}{nr_b^{2+n/2}\left(1+\frac{m}{2r_b}\right)^3}\left[\frac{m}{2}-r_b\left(1-\frac{n}{2}-\frac{mn}{4r_b}\right)\right], \tag{60}$$

$$A_2=\frac{1}{r_b^{2-n/2}\left(1+\frac{m}{2r_b}\right)^3}\left[-\frac{m}{2n}+r_b\left(\frac{1}{2}+\frac{1}{n}+\frac{m}{4r_b}\right)\right], \tag{61}$$

$$B_{1a}=\frac{-4r_b^2\left(1-\frac{2m}{r_b}\right)-m^2+2xr_b^2\left(1-\frac{m^2}{4r_b^2}\right)}{4xr_b^{3+x/2}\left(1+\frac{m}{2r_b}\right)^4}, \tag{62}$$

$$B_{2a}=\frac{4r_b^2\left(1-\frac{2m}{r_b}\right)+m^2+2xr_b^2\left(1-\frac{m^2}{4r_b^2}\right)}{4xr_b^{3-x/2}\left(1+\frac{m}{2r_b}\right)^4}, \tag{63}$$

$$B_{1b}=\frac{1}{4r_b^3\left(1+\frac{m}{2r_b}\right)^4}\left[4r_b^2-m^2+(m^2-8mr_b+4r_b^2)\ln(r_b)\right], \tag{64}$$

$$B_{2b}=-\frac{m^2-8mr_b+4r_b^2}{4r_b^3\left(1+\frac{m}{2r_b}\right)^4}. \tag{65}$$

V_{2a} has its maximum at $r=r_b$, and V_{2b} at $r=0$.

Using Eq. (52)–(54) in Eq. (3)–(6), we get the expressions for the energy density, pressure and sound velocity

of the disk:

$$\sigma = \frac{a}{4\pi}\left[A_1(2+n)\mathcal{R}^{-1/2+n/4} + A_2(2-n)\mathcal{R}^{-1/2-n/4}\right], \tag{66}$$

$$\begin{aligned} P_{2a} = &-\frac{a}{8\pi\left(B_{1a}\mathcal{R}^{1/2+x/4} + B_{2a}\mathcal{R}^{1/2-x/4}\right)}\left[B_{1a}A_1(2+2n-x)\mathcal{R}^{(x+n)/4}\right. \\ &+B_{1a}A_2(2-2n-x)\mathcal{R}^{(x-n)/4} + B_{2a}A_1(2+2n+x)\mathcal{R}^{(-x+n)/4} \\ &\left.+B_{2a}A_2(2-2n+x)\mathcal{R}^{-(x+n)/4}\right], \end{aligned} \tag{67}$$

$$\begin{aligned} P_{2b} = &-\frac{a}{4\pi[2B_{1b} + B_{2b}\ln(\mathcal{R})]}\left\{2(1+\sqrt{2})B_{1b}A_1\mathcal{R}^{-1/2+\sqrt{2}/4}\right. \\ &+2(1-\sqrt{2})B_{1b}A_2\mathcal{R}^{-1/2-\sqrt{2}/4} + \left[(1+\sqrt{2})\ln(\mathcal{R}) - 2\right]B_{2b}A_1\mathcal{R}^{-1/2+\sqrt{2}/4} \\ &\left.+\left[(1-\sqrt{2})\ln(\mathcal{R}) - 2\right]B_{2b}A_2\mathcal{R}^{-1/2-\sqrt{2}/4}\right\}, \end{aligned} \tag{68}$$

$$\begin{aligned} V_{2a}^2 = &\frac{1}{2(4-n^2)\left[A_2 + A_1\mathcal{R}^{n/2}\right]\left[B_{2a} + B_{1a}\mathcal{R}^{x/2}\right]^2}\left\{A_1\mathcal{R}^{n/2}\right. \\ &\left[B_{1a}^2(n-2)(2n-x+2)\mathcal{R}^x + B_{2a}^2(n-2)(2n+x+2)\right. \\ &\left.-4B_{1a}B_{2a}(-n^2+n+x^2+2)\mathcal{R}^{x/2}\right] + A_2\left[B_{1a}^2(n+2)(2n+x-2)\mathcal{R}^x\right. \\ &\left.\left.+B_{2a}^2(n+2)(2n-x-2) - 4B_{1a}B_{2a}(-n^2-n+x^2+2)\mathcal{R}^{x/2}\right]\right\}, \end{aligned} \tag{69}$$

$$\begin{aligned} V_{2b}^2 = &-\frac{2B_{1b} + 2B_{2b} + B_{2b}\ln(\mathcal{R})}{2[2B_{1b} + B_{2b}\ln(\mathcal{R})]^2[A_2 + A_1\mathcal{R}^{1/\sqrt{2}}]}\left\{\left[\sqrt{2}\ln(\mathcal{R}) - 4\right]\right. \\ &\left.\times B_{2b}A_1\mathcal{R}^{1/\sqrt{2}} - \left[\sqrt{2}\ln(\mathcal{R}) + 4\right]B_{2b}A_2 + 2\sqrt{2}B_{1b}\left[A_1\mathcal{R}^{1/\sqrt{2}} - A_2\right]\right\}, \end{aligned} \tag{70}$$

where $\mathcal{R} = R^2 + a^2$. The curves of σ, P and V as function of $\tilde{R} = R/m$ with parameters $n = 1.8$; $m = 0.5$; $r_b = 2$ and $a = 0.5$, 1.0,1.5 are displayed in figure 14 (a) – (c), respectively. Figure 15 (a) – (b) shows the density ρ, pressure p and velocity of sound V for the halo with parameters $n = 1.8$; $m = 0.5$; $r_b = 2$, for $a = 0.5$ along the axis z. The same physical quantities are shown in figures 17 and 18 with $n = \sqrt{2}$.

The tangential velocity v_c is given by

$$\mathrm{v}_{c2a}^2 = R^2\frac{A_2[B_{1a}(n+x)\mathcal{R}^{x/2} + B_{2a}(n-x)] - A_1\mathcal{R}^{n/2}[B_{1a}(n-x)\mathcal{R}^{x/2} + B_{2a}(n+x)]}{[B_{1a}\mathcal{R}^{x/2} + B_{2a}][A_1\mathcal{R}^{n/2}(2a^2 - nR^2) + A_2(2a^2 + nR^2)]}, \tag{71}$$

$$\mathrm{v}_{c2b}^2 = R^2\frac{A_2[2\sqrt{2}B_{1b} + B_{2b}(4+\sqrt{2}\ln(\mathcal{R}))] - A_1\mathcal{R}^{\sqrt{2}/2}[2\sqrt{2}B_{1b} + B_{2b}(-4+\sqrt{2}\ln(\mathcal{R}))]}{[2B_{1b} + B_{2b}\ln(\mathcal{R})][A_1\mathcal{R}^{\sqrt{2}/2}(2a^2 - \sqrt{2}R^2) + A_2(2a^2 + \sqrt{2}R^2)]}, \tag{72}$$

and the specific angular momentum h

$$\begin{aligned} h_{2a} = &\frac{R^2\mathcal{R}^{-1/2+n/4}}{(A_1\mathcal{R}^{n/2} + A_2)^{3/2}\sqrt{B_{1a}(2a^2 - xR^2)\mathcal{R}^{x/2} + B_{2a}(2a^2 + xR^2)}}\times \\ &\left\{A_2[B_{1a}(n+x)\mathcal{R}^{x/2} + B_{2a}(n-x)] - A_1\mathcal{R}^{n/2}[B_{1a}(n-x)\mathcal{R}^{x/2} + B_{2a}(n+x)]\right\}^{1/2}, \end{aligned} \tag{73}$$

$$\begin{aligned} h_{2b} = &\frac{R^2\mathcal{R}^{-1/2+\sqrt{2}/4}}{[A_1\mathcal{R}^{\sqrt{2}/2} + A_2]^{3/2}\sqrt{4a^2B_{1b} + 2B_{2b}[-2R^2 + a^2\ln(\mathcal{R})]}}\times \\ &\left\{A_2[2\sqrt{2}B_{1b} + B_{2b}(4+\sqrt{2}\ln(\mathcal{R}))] - A_1\mathcal{R}^{\sqrt{2}/2}[2\sqrt{2}B_{1b} + B_{2b}(-4+\sqrt{2}\ln(\mathcal{R}))]\right\}^{1/2}. \end{aligned} \tag{74}$$

In figure 16 (a)–(b), the curves of tangential velocities Eq. (71) and $h\frac{dh}{d\tilde{R}}$ Eq. (73), respectively, are displayed as functions of $\tilde{R} = R/m$ with $n = 1.8$; $m = 0.5$; $r_b = 2$; $a = 0.5$, 1.0,1.5. Figure 19 shows the same quantities with $n = \sqrt{2}$. Unlike solution 2, no unstable circular orbits are present for the disks constructed with these parameters.

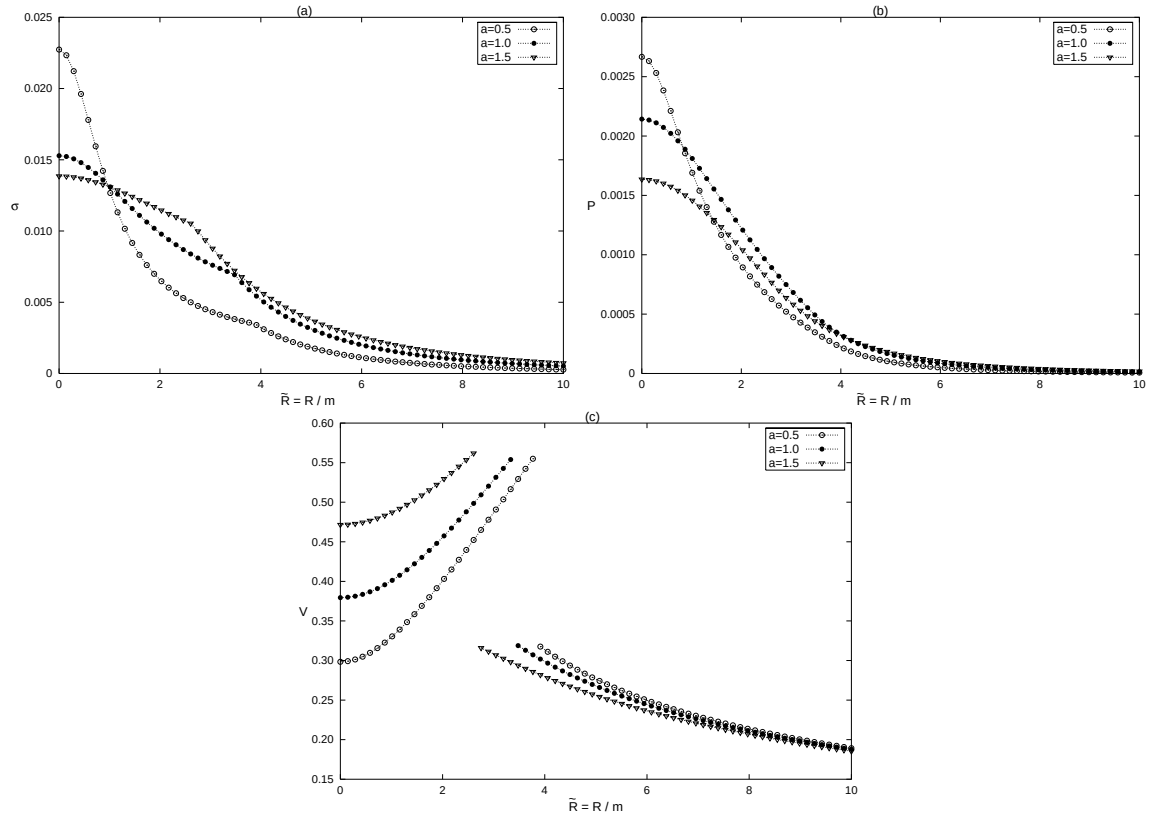

FIG. 14: (a) The surface energy density σ Eq. (66), (b) the pressure P Eq. (67), (c) the velocity of sound V Eq. (69) for the disk with $\mathbf{n} = \mathbf{1.8}$; $m = 0.5$; $r_b = 2$; for $a = 0.5$, 1.0 and 1.5 as function of $\tilde{R} = R/m$.

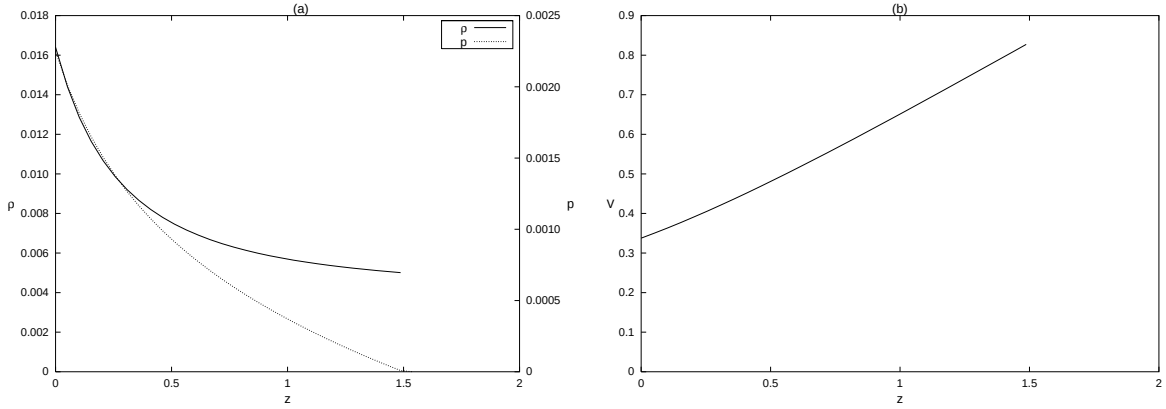

FIG. 15: (a) The density ρ Eq. (55) and pressure p Eq. (56), (b) the velocity of sound V Eq. (58) for the halo with $\mathbf{n} = \mathbf{1.8}$; $m = 0.5$; $r_b = 2$; for $a = 0.5$ along the axis z.

V. DISKS WITH COMPOSITE HALOS FROM SPHERICAL SOLUTIONS

We study two examples of disks with halos constructed from spheres of fluids with two layers as the ones depicted in Fig. 3.

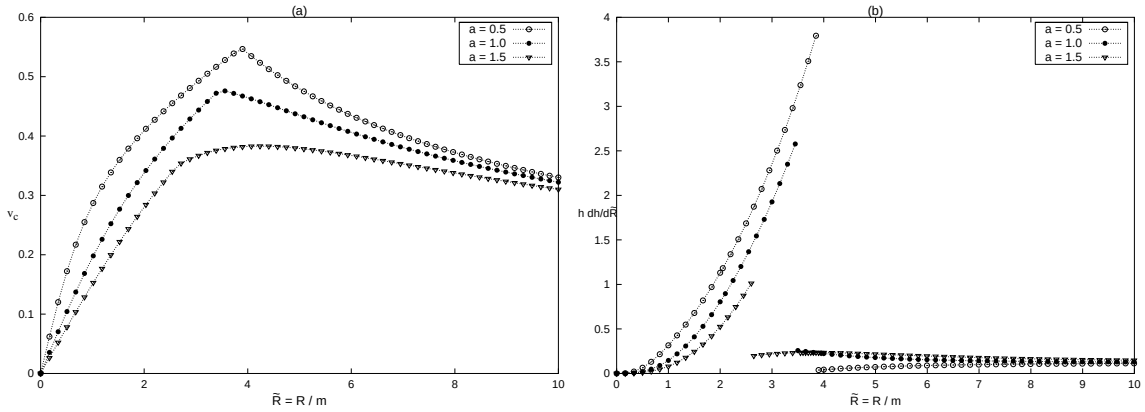

FIG. 16: (a) The tangential velocity v_{ca} Eq. (71), (b) the curves of $h\frac{dh}{d\tilde{R}}$ Eq. (73) with $\mathbf{n = 1.8}$; $m = 0.5$; $r_b = 2$; for $a =$ 0.5, 1.0, and 1.5 as function of $\tilde{R} = R/m$. The disks have no unstable orbits for these parameters.

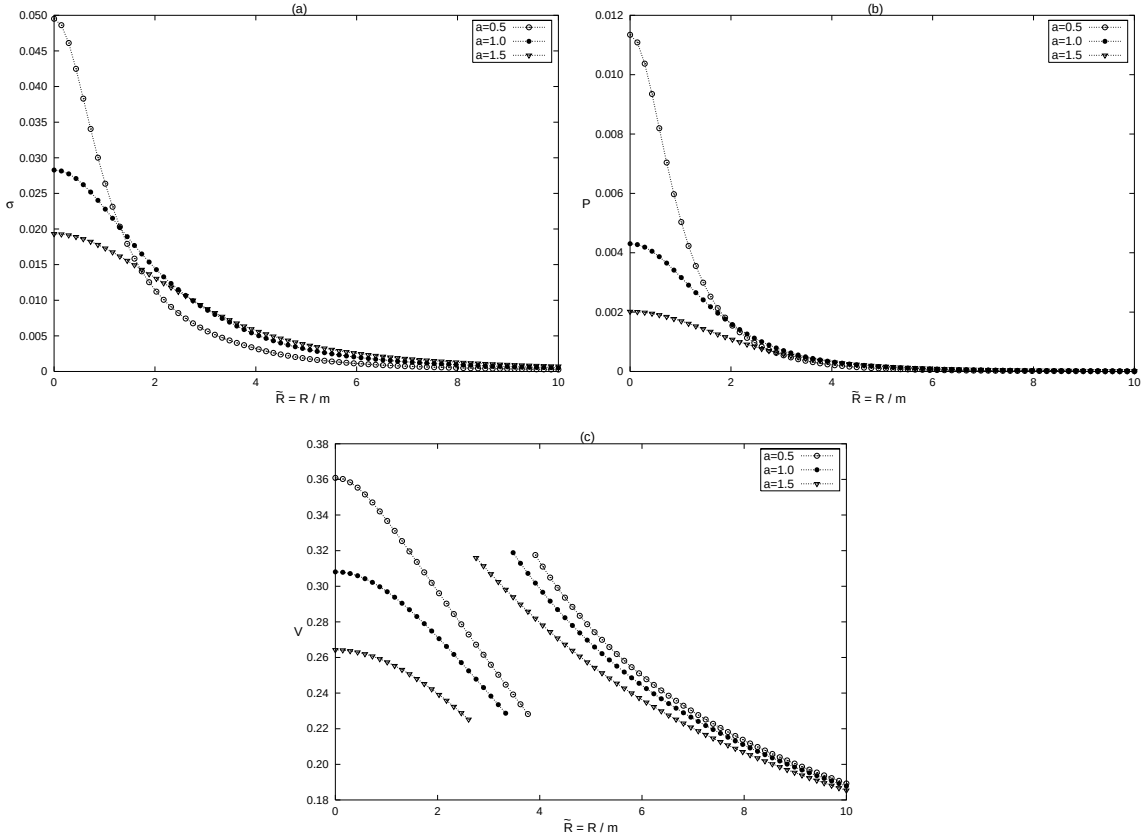

FIG. 17: (a) The surface energy density σ Eq. (66), (b) the pressure P Eq. (68), (c) the velocity of sound V Eq. (70) for the disk with $n = \sqrt{2}$; $r_b = 2$; $m = 0.5$; for $a = 0.5$, 1.0 and 1.5 as function of $\tilde{R} = R/m$.

A. Internal Schwarzschild solution and Buchdahl solution

Let us consider a fluid sphere is formed by two layers: The internal layer, $0 \leq r < r_1$, will be taken as the internal Schwarzschild solution (solution 2a with n=2),

$$e^{\nu} = \frac{\left(B_1 r^2 + B_2\right)^2}{\left(A_1 r^2 + A_2\right)^2}, \quad e^{\lambda} = \frac{1}{\left(A_1 r^2 + A_2\right)^2}. \tag{75}$$

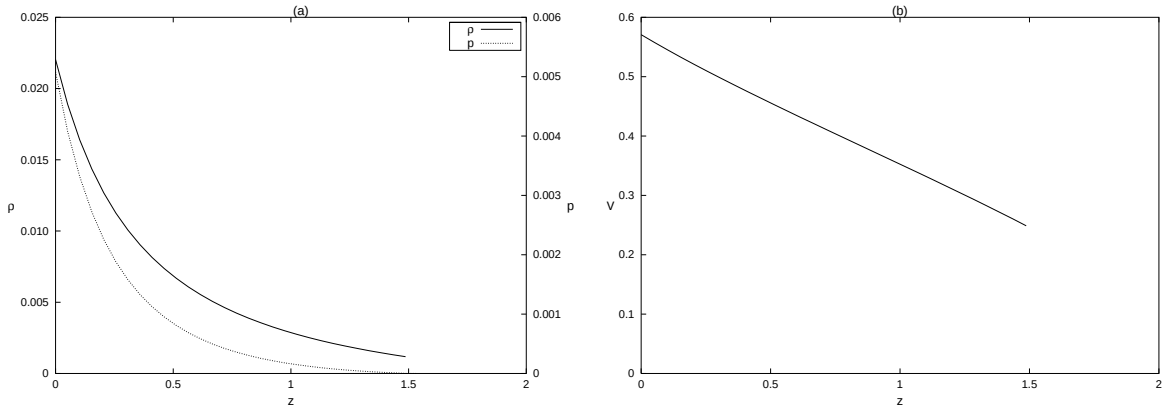

FIG. 18: (a) The density ρ Eq. (55) and pressure p Eq. (57), (b) the velocity of sound V Eq. (59) for the halo with $n = \sqrt{2}$; $r_b = 2$; for $a = 0.5$ along the axis z.

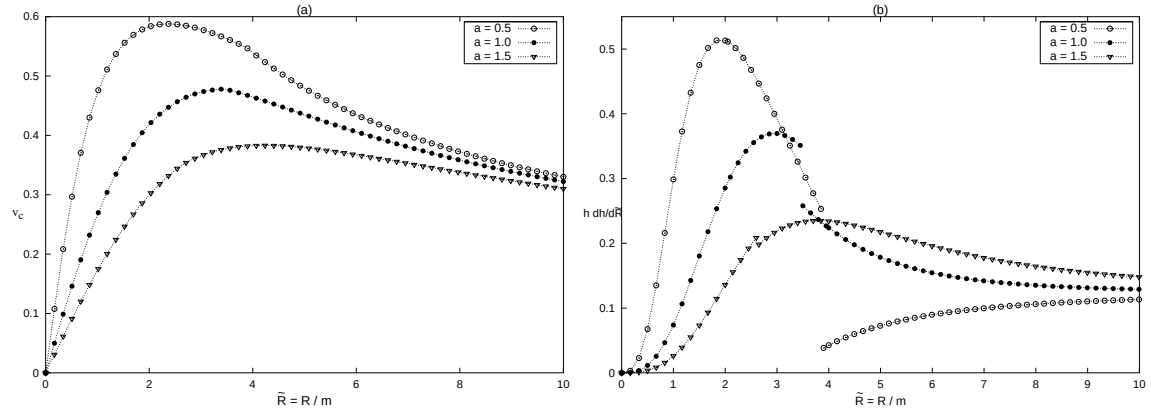

FIG. 19: (a) The tangential velocity v_{cb} Eq. (72), (b) The curves of $h\frac{dh}{d\tilde{R}}$ Eq. (74) with $n = \sqrt{2}$; $m = 0.5$; $r_b = 2$; for $a = 0.5$, 1.0, and 1.5 as function of $\tilde{R} = R/m$. The disks have no unstable orbits for these parameters.

The external layer, $r > r_1$ is taken as the Buchdahl solution,

$$e^{\nu} = \left(\frac{1 - \frac{C}{\sqrt{1+kr^2}}}{1 + \frac{C}{\sqrt{1+kr^2}}}\right)^2, \quad e^{\lambda} = \left(1 + \frac{C}{\sqrt{1+kr^2}}\right)^4. \tag{76}$$

Note that the external layer has no boundary, i.e., this layer has infinite radius.

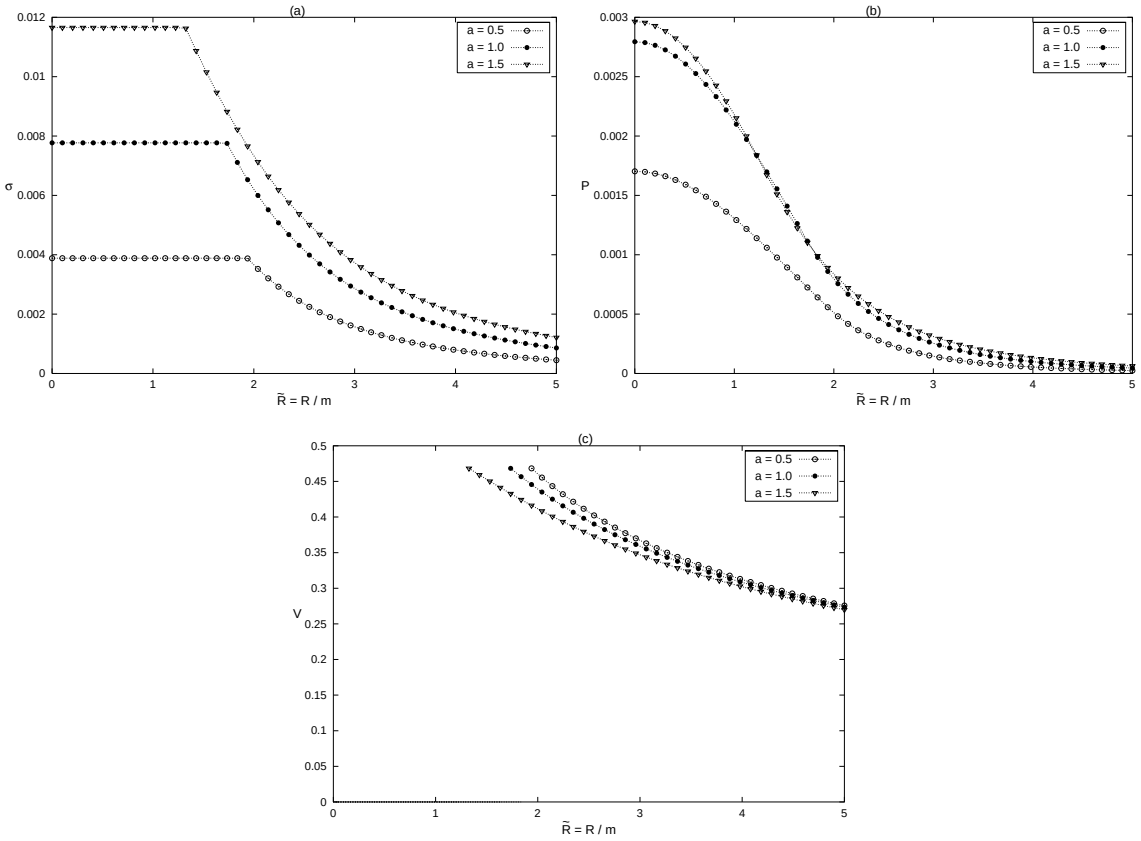

FIG. 20: (a) The surface energy density σ, (b) the pressure P, (c) the velocity of sound V for the disk generated from spherical fluid layers Eq. (75)–(76) with $m = 1$; $k = 1$; $r_1 = 2$; for $a = 0.5$, 1.0 and 1.5 as function of $\tilde{R} = R/m$.

According to the continuity conditions at $r = r_1$, the constants are related through:

$$A_1 = \frac{Ck}{\left(C + \sqrt{1 + kr_1^2}\right)^3}, \quad A_2 = \frac{1 + \frac{C}{(1+kr_1^2)^{3/2}}}{\left(1 + \frac{C}{\sqrt{1+kr_1^2}}\right)^3}, \tag{77}$$

$$B_1 = \frac{Ck}{(1 + kr_1^2)\left(1 + \frac{C}{\sqrt{1+kr_1^2}}\right)^3} D, \tag{78}$$

$$D = \frac{\left[C(1 - 3kr_1^2) - \frac{C^2}{\sqrt{1+kr_1^2}}(1 - kr_1^2) + 2(1 + kr_1^2)^{3/2}\right]}{\left[(1 + kr_1^2)^2 + 2C\sqrt{1 + kr_1^2} + C^2(1 - kr_1^2)\right]}, \tag{79}$$

$$B_2 = \frac{1 - \frac{C}{\sqrt{1+kr_1^2}}}{\left(1 + \frac{C}{\sqrt{1+kr_1^2}}\right)^3} - B_1 r_1^2. \tag{80}$$

With these relations, one verifies that, using Eq. (27) and Eq. (66), Eq. (28) and Eq. (67), both the energy density and the pressure are continuous at the radius $R = \sqrt{r_1^2 - a^2}$ of the disk.

Figure 20 (a)–(c) shows, respectively, σ, P and V for the disk obtained from fluid layers Eq. (75)–(76) with parameters $m = 1$; $k = 1$; $r_1 = 2$; for $a = 0.5$, 1.0 and 1.5 as function of $\tilde{R} = R/m$. The density ρ, pressure p and velocity of sound V for the halo along the z axis with the same parameters for $a = 0.5$ is shown in figure 21.

In figure 22 (a)–(b), the curves of tangential velocities and of $h\frac{dh}{d\tilde{R}}$, respectively, are displayed as functions of $\tilde{R} = R/m$.

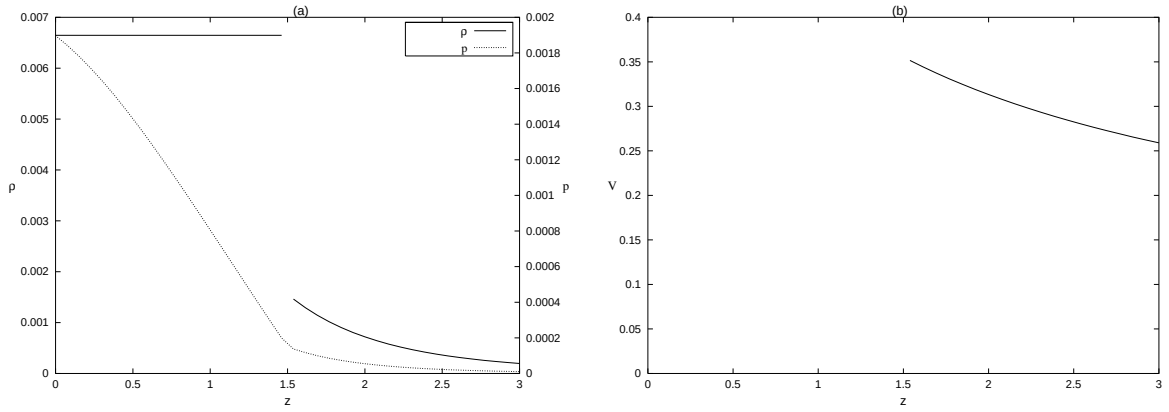

FIG. 21: (a) The density ρ and pressure p, (b) the velocity of sound V for the halo formed by fluid layers Eq. (75)–(76) with $m = 1$; $k = 1$; $r_1 = 2$ and $a = 0.5$ along the axis z.

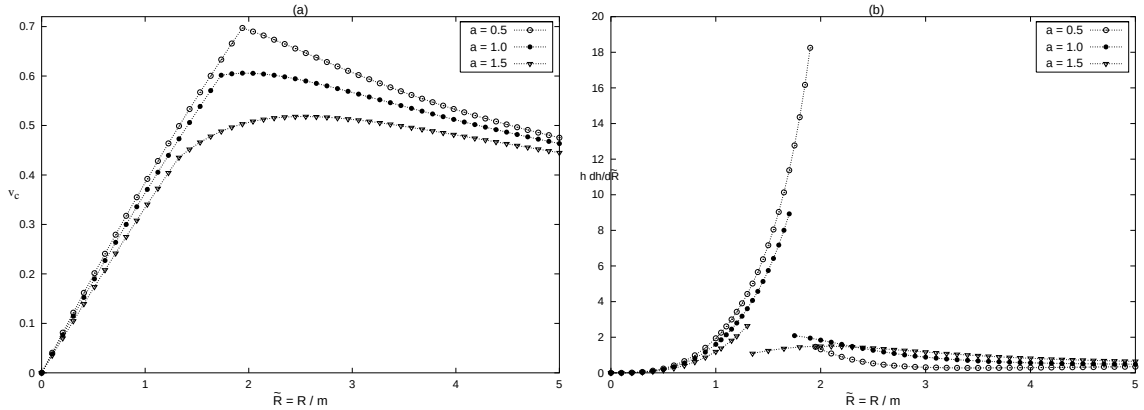

FIG. 22: (a) The tangential velocity v_c, (b) the curves of $h\frac{dh}{d\tilde{R}}$ for the disk generated from fluid layers Eq. (75)–(76) with $m = 1$; $k = 1$; $r_1 = 2$; for $a = 0.5$, 1.0 and 1.5 as function of $\tilde{R} = R/m$. The disks obtained with these parameters have no unstable orbits.

B. NPV Solution 2b with $n = \sqrt{2}$ and NPV solution 1b with $k = -2 + \sqrt{2}$

Now we consider a sphere composed with two finite layers: The internal layer, $0 \leq r < r_1$, is taken as the NPV solution 2b with $n = \sqrt{2}$,

$$e^{\nu} = \frac{\left(B_1 + B_2 \ln(r)\right)^2}{\left(A_1 r^{\sqrt{2}/2} + A_2 r^{-\sqrt{2}/2}\right)^2}, \quad e^{\lambda} = \frac{1}{\left(A_1 r^{1+\sqrt{2}/2} + A_2 r^{1-\sqrt{2}/2}\right)^2}. \tag{81}$$

The external layer, $r_1 < r < r_2$, is taken as the NPV solution 1b with $k = -2 + \sqrt{2}$,

$$e^{\nu} = r^{\sqrt{2}} \left(A_3 + B_3 \ln(r)\right)^2, \quad e^{\lambda} = C r^{-2+\sqrt{2}}. \tag{82}$$

The spacetime outside the sphere, $r > r_2$, will be taken as the Schwarzschild's vacuum solution is isotropic coordinates.

$$e^{\nu} = \frac{\left(1 - \frac{m}{2r}\right)^2}{\left(1 + \frac{m}{2r}\right)^2}, \quad e^{\lambda} = \left(1 + \frac{m}{2r}\right)^4. \tag{83}$$

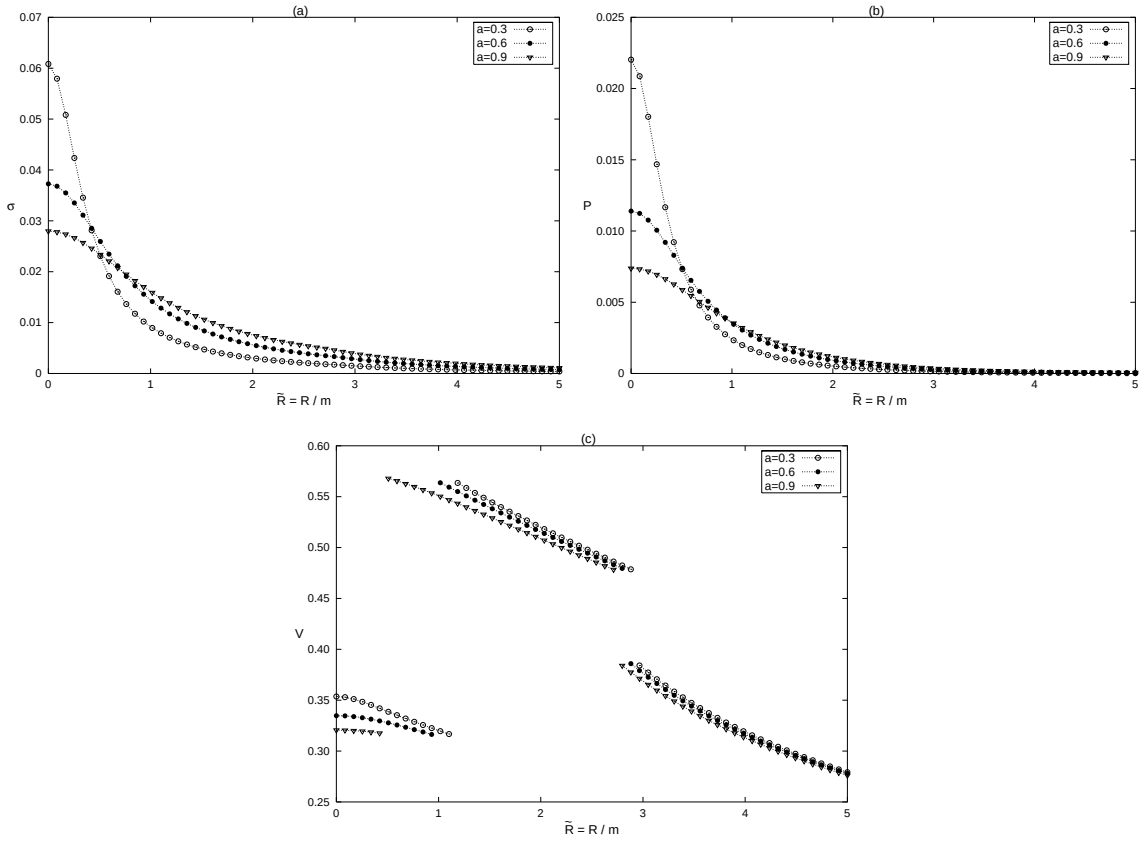

FIG. 23: (a) The surface energy density σ, (b) the pressure P, (c) the velocity of sound V for the disk generated from spherical fluid layers Eq. (81)–(82) with $r_1 = 1$; $r_2 = 2$; for $a = 0.3$, 0.6 and 0.9 as function of $\tilde{R} = R/m$.

In this case the pressure should be zero at $r = r_2$. The continuity conditions at $r = r_1$ and $r = r_2$ give the relations:

$$\frac{m}{r_2} = \frac{\sqrt{2}(2-\sqrt{2})}{1+\sqrt{2}},\ C = \frac{64 r_2^{2-\sqrt{2}}}{(1+\sqrt{2})^4},\ B_3 = \frac{1}{4 r_2^{1/\sqrt{2}}},\ A_3 = -\frac{2\sqrt{2}+\ln(r_2)}{r_2^{1/\sqrt{2}}}, \tag{84}$$

$$A_1 = 0,\ A_2 = \frac{1}{\sqrt{C}},\ B_2 = \frac{r_1^{\sqrt{2}}}{2\sqrt{2C}}\left[(A_3 + B_3\ln(r_1))\,(1 - r_1^{-\sqrt{2}}) + 2\sqrt{2}B_3\right], \tag{85}$$

$$B_1 = \frac{r_1^{\sqrt{2}}}{2\sqrt{2C}}\left[(A_3 + B_3\ln(r_1))\left(2\sqrt{2}r_1^{-\sqrt{2}} - \ln(r_1) + \ln(r_1) r_1^{-\sqrt{2}}\right) - 2\sqrt{2}B_3\ln(r_1)\right]. \tag{86}$$

Using Eq. (43) and Eq. (66), the energy density of the disk at $R = \sqrt{r_1^2 - a^2}$ is continuous, but not the pressure. The difference between Eq. (68) and Eq. (45) is

$$\Delta P = \frac{a(r_1^{\sqrt{2}/2} - r_1^{-\sqrt{2}/2})}{16\pi\sqrt{C} r_1 (A_3 + B_3\ln(r_1))}\left[\sqrt{2}(A_3 + B_3\ln(r_1)) + 4B_3\right]. \tag{87}$$

The pressure is continuous if $r_1^{\sqrt{2}/2} - r_1^{-\sqrt{2}/2} = 0 \to r_1 = 1$.

Figure 23 (a)–(c) shows, respectively, σ, P and V for the disk obtained from fluid layers (81)–(82) with parameters $r_1 = 1$; $r_2 = 2$; for $a = 0.3$, 0.6 and 0.9 as function of $\tilde{R} = R/m$. The density ρ, pressure p and velocity of sound V for the halo along the z axis with the same parameters for $a = 0.3$ is shown in figure 24.

In figure 25 (a)–(b), the curves of tangential velocities and of $h\frac{dh}{d\tilde{R}}$, respectively, are displayed as functions of $\tilde{R} = R/m$. In this case, regions of unstable orbits exist for parameters $a = 0.3$ and $a = 0.6$.

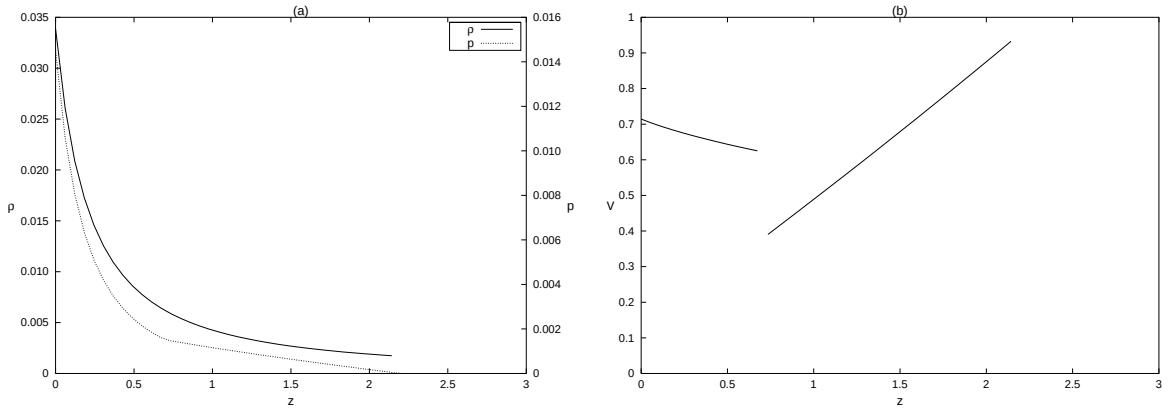

FIG. 24: (a) The density ρ and pressure p, (b) the velocity of sound V for the halo formed by fluid layers Eq. (81)–(82) with $r_1 = 1$; $r_2 = 2$ and $a = 0.3$ along the axis z.

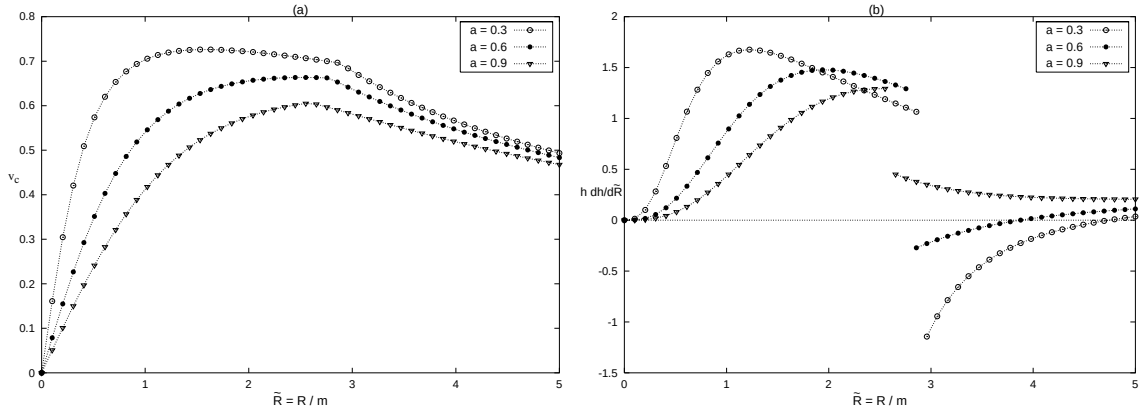

FIG. 25: (a) The tangential velocity v_c, (b) the curves of $h\frac{dh}{d\tilde{R}}$ for the disk generated from spherical fluid layers Eq. (81)–(82) with $r_1 = 1$; $r_2 = 2$; for $a = 0.3$, 0.6 and 0.9 as function of $\tilde{R} = R/m$. Regions of unstable circular orbits appear for the disks obtained with parameters $a = 0.3$ and 0.6.

VI. DISCUSSION

The "displace, cut and reflect" method applied to solutions of Einstein field equations in isotropic coordinates can generate disks with positive energy density and equal radial and azimuthal pressures (perfect fluid). With solutions of static spheres of perfect fluid it is possible to construct disks of perfect fluid surrounded also by perfect fluid matter. As far we know these are the first disk models of this kind in the literature.

All disks constructed as examples have some common features: surface energy density and pressures decrease monotonically and rapidly with radius. As the "cut" parameter a decreases, the disks become more relativistic, with surface energy density and pressure more concentrated near the center. Also regions of unstable circular orbits are more likely to appear for high relativistic disks. Parameters can be chosen so that the sound velocity in the fluid and the tangential velocity of test particles in circular motion are less then the velocity of light. This tangential velocity first increases with radius and reaches a maximum. Then, for large radii, it decreases as $1/\sqrt{R}$, in case of disks generated from Schwarzschild and Buchdahl's solutions. The sound velocity is also a decreasing function of radius, except in solution NPV 2a with $\sqrt{2} < n \leq 2$, where it reaches its maximum value at the boundary. In principle other solutions of static spheres of perfect fluid could be used to generate other disk + halo configurations, but it is not guaranteed that the disks will have the characteristics of normal fluid matter.

We believe that the presented disks can be used to describe more realistic model of galaxies than most of the already studied disks since the counter rotation hypothesis is not needed to have a stable configuration.

We want to finish our discussion by presenting a table that summarizes our results about disks in an unify manner.

Disks properties

Solution	**metric coefficients**	**matching conditions**	**energy density**	**pressure**	**sound velocity**	**angular momentum**
External Schwarzschild	(9)	–	(10)	(11)	(13)	(23)
Buchdahl	(24)	–	(27)	(28)	(29)	(31)
NPV 1a	(32)–(33)	(40)–(41)	(43)	(44)	(46)	(50)
NPV 1b	(32), (34)	(40), (42)	(43)	(45)	(47)	(51)
NPV 2a	(52)–(53)	(60)–(63)	(66)	(67)	(69)	(73)
NPV 2b	(52), (54)	(60)–(61), (64)–(65)	(66)	(68)	(70)	(74)
Internal Schwarzschild +Buchdahl	(75)–(76)	(77)–(80)	(66), (27)	(67), (28)	(69), (29)	(73), (31)
NPV 2b+NPV 1b +external Schwarzschild	(81), (82), (83)	(84)–(86)	(66), (43), (10)	(68), (45), (11)	(70), (47), (13)	(74), (51), (23)

In the table we list the seed metric coefficients, matching conditions at the boundaries and relevant physical quantities of all disks studied in this work. The numbers refer to the equations presented along the paper and NPV stands for Narlikar, Patwardhan and Vaidya as before.

Acknowledgments

We want to thank FAPESP, CAPES and CNPQ for financial support.

[1] W. A. Bonnor and A. Sackfield, *Commun. Math. Phys.* **8**, 338 (1968).
[2] T. Morgan and L. Morgan, *Phys. Rev.* **183**, 1097 (1969).
[3] L. Morgan and T. Morgan, *Phys. Rev. D* **2**, 2756 (1970).
[4] G. González and P. S. Letelier, *Class. Quantum Grav.* **16**, 479 (1999).
[5] T. Ledvinka, M. Zofka, and J. Bičák, in *Proceedings of the 8th Marcel Grossman Meeting in General Relativity*, edited by T. Piran (World Scientific, Singapore, 1999), pp. 339-341.
[6] P. S. Letelier, *Phys. Rev. D* **60**, 104042 (1999).
[7] J. Katz, J. Bičák, and D. Lynden-Bell, *Class. Quantum Grav.* **16**, 4023 (1999).
[8] D. Lynden-Bell and S. Pineault, Mon. Not. R. Astron. Soc. 185, 679 (1978)
[9] J. P. S. Lemos, Class. Quan. Grav. 6, 1219 (1989)
[10] J. P. S. Lemos and P. S. Letelier, Class. Quan. Grav. 10, L75 (1993)
[11] J. P. S. Lemos and P. S. Letelier, Phys. Rev D49, 5135 (1994)
[12] J. P. S. Lemos and P. S. Letelier, Int. J. Mod. Phys. D5, 53 (1996)
[13] C. Klein, Class. Quan. Grav. 14, 2267 (1997)
[14] J. Bičák, D. Lynden-Bell and J. Katz, Phys. Rev. D47, 4334 (1993)
[15] J. Bičák, D. Lynden-Bell and C. Pichon, Mon. Not. R. Astron. Soc. 265, 126 (1993)
[16] O. Semerák, *Towards gravitating disks around stationary black holes*, (April, 2002), available at http://xxx.lanl.gov/abs/gr-qc/0204025.
[17] G. G. Kuzmin, *Astron. Zh.*, **33**, 27 (1956).
[18] A. H. Taub, J. Math. Phys. 21, 1423 (1980)
[19] J.P.S. Lemos and P.S. Letelier, Phys Lett. A 153, 288 (1991).
[20] Lord Rayleigh, Proc. R. Soc. Lond. Ser. A 93, 148 (1916).
[21] L. D. Landau, E. M. Lifshitz, *Fluid Mechanics*, 2nd Ed. (Pergamon Press, Oxford, 1987), §27.
[22] B. Kuchowicz, *Acta Phys. Pol.*, **B** 3, 209 (1972).
[23] H. A. Buchdahl, *Astrophys. J.*, **140**, 1512 (1964).
[24] V. V. Narlikar, G. K. Patwardhan, P. C. Vaidya, *Proc. Natl. Inst. Sci. India*, **9**, 229 (1943).